Calhoun
Institutional Archive of the Naval Postgraduate School

Calhoun: The NPS Institutional Archive

Theses and Dissertations | Thesis Collection

1970

Application of the fast Fourier system to the computation of electric fields and associated heating patterns in human tissue.

Schaefer, Edward Michael

University of Washington

DUDLEY KNOX LIBRARY

http://www.nps.edu/library

Calhoun is a project of the Dudley Knox Library at NPS, furthering the precepts and goals of open government and government transparency. All information contained herein has been approved for release by the NPS Public Affairs Officer.

Dudley Knox Library / Naval Postgraduate School
411 Dyer Road / 1 University Circle
Monterey, California USA 93943

APPLICATION OF THE FAST FOURIER SYSTEM TO THE COMPUTATION OF ELECTRIC FIELDS AND ASSOCIATED HEATING PATTERNS IN HUMAN TISSUE.

Edward Micheal Schaefer

Gaylord
CASE BINDER
Syracuse, N. Y.
Stockton, Calif.

LIBRARY
NAVAL POSTGRADUATE SCHOOL
MONTEREY, CALIF. 93940

APPLICATION OF THE FAST FOURIER TRANSFORM TO THE COMPUTATION OF ELECTRIC FIELDS AND ASSOCIATED HEATING PATTERNS IN HUMAN TISSUE

by

EDWARD MICHEAL SCHAEFER

A thesis submitted in partial fulfillment
of the requirements for the degree of

MASTER OF SCIENCE IN ELECTRICAL ENGINEERING

UNIVERSITY OF WASHINGTON

1970

Approved by _____
(Chairman of Supervisory Committee)

Department _____
(Departmental Faculty sponsoring candidate)

Date _____

LIBRARY
NAVAL POSTGRADUATE SCHOOL
MONTEREY, CALIF. 93940

In presenting this thesis in partial fulfillment of the requirements for an advanced degree at the University of Washington I agree that the Library shall make it freely available for inspection. I further agree that permission for extensive copying of this thesis for scholarly purposes may be granted by my major professor, or, in his absence, by the Director of Libraries. It is understood that any copying or publication of this thesis for financial gain shall not be allowed without my written permission.

Signature_____

Date_____

TABLE OF CONTENTS

APPENDICES

LIST OF FIGURES

LIST OF FIGURES

LIST OF TABLES

UNIVERSITY OF WASHINGTON

ABSTRACT

APPLICATION OF THE FAST FOURIER TRANSFORM TO THE COMPUTATION OF ELECTRIC FIELDS AND ASSOCIATED HEATING PATTERNS IN HUMAN TISSUE

by

EDWARD MICHEAL SCHAEFER

Chairman of Supervisory Committee: David L. Johnson
Department of Electrical Engineering

Relative heating in human tissue is defined in terms of the electric fields. Analytical expressions for the electric fields in planar layers of human tissue due to a known aperture distribution at the surface of the tissue are derived. The Cooley-Tukey algorithm for efficient computation of discrete Fourier transforms is illustrated for a one-dimensional problem. Flow charts for the use of the fast Fourier transform (FFT) in relative heating problems are developed. Results from computation of relative heating by the FFT are compared to similar results obtained by the Guassian quadrature transformation procedure.

ACKNOWLEDGMENTS

The author gratefully acknowledges the invaluable technical advice and constructive criticism of Assistant Professor A. W. Guy of the Department of Physical Medicine and Rehabilitation and the help and moral support of Professor D. L. Johnson of the Department of Electrical Engineering. The author also wishes to acknowledge the financial assistance of the Social Rehabilitation Service Grant RT-3 and the Bioengineering Project, National Institute of General Medical Science Division of the National Institute of Health.

A special note of thanks is due Mr. John M. McDougal for his assistance in programming and to Miss Linda K. Johnson for her patient preparation of the manuscript. Finally, the author wishes to thank his wife, Linda I. Schaefer, for her kind understanding and encouragement throughout the entire research project.

CHAPTER 1

INTRODUCTION

1.1 Our Changing Environment

More technological advances have been made in the Twentieth Century than in all of man's past history. These advances have affected nearly every aspect of existence on this planet as well as fulfilling the age-old dream of setting foot on other heavenly bodies. Man, as a result, enjoys a longer and easier life.

These phenomenal advances have not been made without some potentially harmful side effects to the environment. Factories have contributed to air and water pollution. Questions are being raised about the relative merits of supersonic travel versus the adverse effects of the resultant sonic boom. Every man has a car in his garage but the countryside is being ruined by ribbons of concrete. Many recent discussions have centered on the adverse effects of electromagnetic and particulate radiation on biological systems in general and human tissue in particular, but there are also many advantageous uses for electromagnetic and particulate radiation such as the use of electromagnetics in diathermy treatment of many musculoskeletal disorders and the use of nuclear energy to generate electric energy.

1.2 Heat for Therapy

Man has searched for more effective methods of applying heat to his body for various aches and pains since he first discovered what the

heat of the sun could do for him.[1] This search has led man to investigate nearly every method of heat production including the sun, hot water, infrared radiation, ultrasonics and electromagnetic radiation. In recent years, there have been many reports[2] of successful applications of electromagnetic heating of deep body tissue for therapeutic purposes (diathermy).

Since diathermy has proven to be effective for treatment of many musculoskeltetal disorders, the search is continuing in the Department of Physical Medicine and Rehabilitation at the University of Washington[3, 4, 5] in an effort to find the most efficient method of realizing deep tissue heating without damaging the skin and subcutaneous fat.

Computer solutions of the mathematical models of the diathermy problem have in the past been confined to investigating only a rather limited set of points in the volume of the models. This research will investigate an algorithm which can more efficiently provide a much more complete picture of the heating.

A direct consequence of diathermy research will be the development of the analytic methods which can be used in the study of the adverse effects of electromagnetic radiation and as a quantitative aid in the establishment of radiation safety standards.

1.3 Radiation Safety Standards

The relative importance of determining the biological effects of electromagnetic radiation can be ascertained by the attention given to the problem in recent years:

a. Numerous congressional hearings were held on the subject in 1967 and 1968.[6, 7]

b. The Radiation Control for Health and Safety Act of 1968[8] (RCHSA-1968) was enacted as a result of the congressional hearings.

c. The Armed Forces have, since 1957, held an annual Tri-Service Conference on the Biological effects of Microwave Radiating Equipments.[9]

d. There is continuing research into the possible uses of electromagnetic radiation in the field of medicine.

e. There has been a great deal of research conducted on the use of electromagnetic heating of deep body tissue for therapeutic purposes (diathermy).[3, 4, 5, 10]

Discussion and research into the biological effects of electromagnetic radiation have resulted in both the United States and the USSR accepting radiation safety standards for prolonged exposure to radiation.

1.4 The Need for Research

That there is a need for further research can be evidenced by the fact that the safety standards set by the two countries differ by three orders of magnitude. In fact, the RCHSA-1968[8] directs the Secretary of the Department of Health, Education and Welfare to conduct studies of the problem and report the findings to Congress.

How should the research be conducted? In the past, most of the research on the biological effects of electromagnetic radiation has been

qualitative rather than quantitative. Considerable research has been conducted on animals and the results have been extrapolated to man with a fair amount of success. But in fact, the very question of qualitative versus quantitative research has been debated at great lengths while the proponents of each side continued to conduct the research as best they could in view of the facilities at their disposal.

1.5 An Engineering Approach

A reasonable engineering approach to the problem would incorporate both quantitative and qualitative research in a team effort by engineers and physiologists where members of each discipline would investigate that aspect of the problem to which they are best suited.

The engineers are well suited to investigate the quantitative aspects of the problem by first constructing planar and cylindrical layered models which exhibit the electromagnetic properties of human tissue. This analysis would mainly encompass the problem of determining by analytical methods the electric and magnetic fields within the tissue layers of the models for different internal or external source configurations.

When the models have been developed to the point where they reliably agree with theoretical calculations, the same modelling materials can be used to model the complex geometries of the human body. The answers derived from the models can then be correlated with data from qualitative methods.

1.6 Research Objectives

The approach outlined in the preceding section is currently in use at the University of Washington. The problem under investigation is the determination of the optimum frequency of electromagnetic radiation and applicator configuration to be used for therapeutic heating of deep tissues.

The subject of this particular research is a comparison of the Guassian quadrature and fast Fourier transform (FFT) algorithms used to compute the electric fields induced in planar layers of human tissue. The vehicle problem is the computation of the relative heating pattern arising from a direct contact diathermy applicator. The applicator has a TE_{10} waveguide mode radiating into a bi-layered, semi-infinite lossy medium (See Figure 1.1). A subcutaneous fat layer overlying a semi-infinite muscle is modelled by this medium.

Current analysis utilizes the Gaussian quadrature method to perform the necessary transformations. The economics of computation time in the continuing research program dictate that only a relatively few points in any plane of the tissue can be computed and those must be along an axis of symmetry. The fast Fourier transform will compute an entire array of points in any desired plane, thereby presenting a more complete picture, at a considerable savings on a cost per point basis.

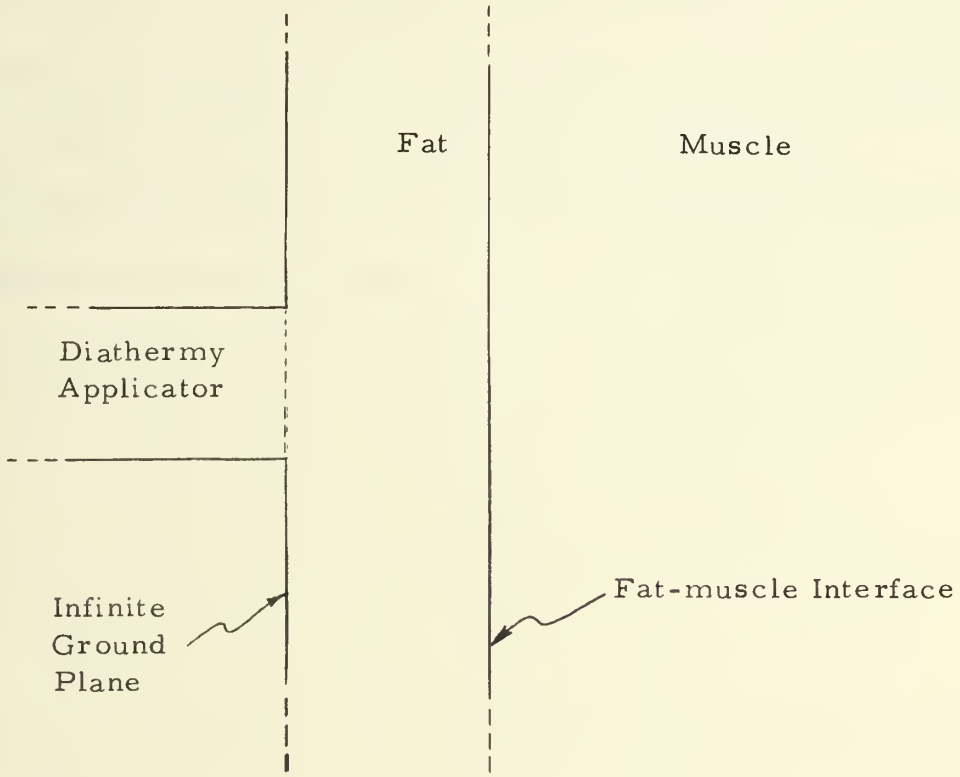

Figure 1.1

Model of Human Tissue

1.7 Content of Succeeding Chapters

In Chapter 2 the electric field equations and relative heating expressions to be solved are developed from the literature. Chapter 3 discusses the fast Fourier transform which will be used to accomplish the inverse transforms required to compute the electric fields for the relative heating patterns.

The use of the FFT in this and another related problem will be presented by discussion and flow diagrams in Chapter 4.

This research project analyzes the merits of using the FFT to compute the electric fields necessary to obtain the relative heating patterns.

The results from the fast Fourier transformations at several frequencies are compared in Chapter 5 to results obtained from Gaussian quadrature transformations already accomplished by Guy and McDougall.[11]

A brief discussion of the conclusions to be drawn from this research is presented in Chapter 6.

CHAPTER 2

RELATIVE HEATING IN PLANAR LAYERS OF HUMAN TISSUE

2.1 Objectives

Relative heating from a rectangular aperture in an infinite conducting plane radiating into a two layered model of human tissue is defined in Section 2.2 (See Figure 2.1). The human tissues modelled are a subcutaneous fat layer of depth z_1 overlying a semi-infinite muscle layer. The succeeding sections develop the necessary electric field equations required for computation of relative heating.

The development of the field expressions follows the approach of Villeneuve[12] and Guy.[13] Villeneuve utilizes the Fourier transform approach in computing the effective input impedance of an open-ended waveguide radiating into a plasma environment. This problem arises in designing communication antennas on high speed reentry vehicles used in space exploration.

Villeneuve, in his work, develops general expressions for the fields exterior to the waveguide; then, he looks at the expressions only at the aperture. Guy extends the expressions of Villeneuve by matching boundary conditions and derives the field expressions necessary to compute relative heating.

2.2 Relative Heating

The criteria for the design of an optimum diathermy applicator for treatment of musculoskeletal disorders is that the heating per unit

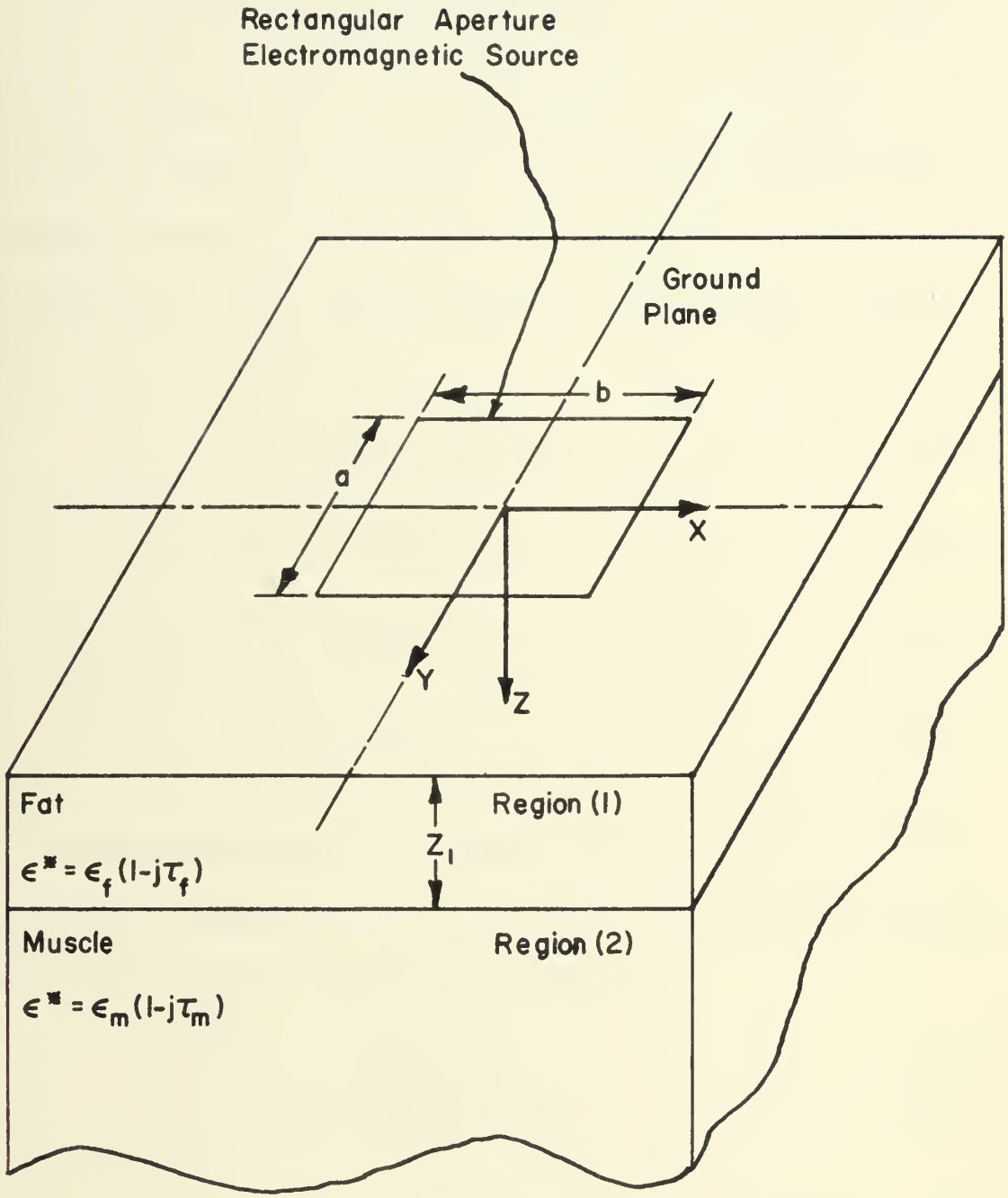

FIGURE 2.1

Tissue Model and Coordinate Definition

volume in the subcutaneous fat be significantly lower than the heating per unit volume in the musculature. The term relative heating arises from this criteria. Relative heating at any point (x, y, z) is defined as the heating per unit volume at the point (x, y, z) relative to the heating per unit volume at the point $(0, 0, z_1)$, where z_1 is the thickness of the subcutaneous fat layer. Guy[3] has shown that the heating per unit volume at the point (x, y, z) is given by

$$W_T = W_x + W_y + W_z \qquad 2.2.1$$

$$W_x = \frac{\sigma}{2} |E_x|^2 \qquad 2.2.2$$

$$W_y = \frac{\sigma}{2} |E_y|^2 \qquad 2.2.3$$

$$W_z = \frac{\sigma}{2} |E_z|^2 \qquad 2.2.4$$

where σ is the conductivity of the medium and the E's are the electric field strengths at the point (x, y, z). From these expressions the relative heating at a point (x, y, z) in the fat layer is given by

$$p_{T_f} = \frac{W_{T_f}(x, y, z)}{W_{T_m}(0, 0, z_1)} \qquad 2.2.5$$

$$p_{T_f} = \frac{\sigma_f}{\sigma_m} \frac{(|E_x|^2 + |E_y|^2 + |E_z|^2)}{(|E_{x0}|^2 + |E_{y0}|^2 + |E_{z1}|^2)} \qquad 2.2.6$$

and in the muscle by

$$p_{T_m} = \frac{W_{T_m}(x, y, z)}{W_{T_m}(0, 0, z_1)} \qquad 2.2.7$$

$$p_{T_m} = \frac{|E_x|^2 + |E_y|^2 + |E_z|^2}{|E_{x0}|^2 + |E_{y0}|^2 + |E_{z1}|^2} \qquad 2.2.8$$

where

$$E_{x0} = E_x(0, 0, z_1) \qquad 2.2.9$$

$$E_{y0} = E_y(0, 0, z_1) \qquad 2.2.10$$

$$E_{z1} = E_z(0, 0, z_1). \qquad 2.2.11$$

The $W_{T_m}(0, 0, z_1)$ which appears in the p_{T_f} and p_{T_m} expressions normalizes the relative heating to unity at the fat-muscle interface.

2.3 General Solution of Electric Fields in Layered Media

In rectangular coordinates, general solutions of the scalar wave equation may be obtained as a linear superposition of plane wave solutions.[10] This process leads to the development of a complete set of Fourier transform pairs which completely specify all of the field components throughout the volume of the fat and muscle.

The electromagnetic fields may be derived from two parallel vector functions whose direction in space is fixed. Assume these functions to be

$$\bar{A} = \bar{U}_x \psi_m \qquad 2.3.1$$

$$\bar{F} = \bar{U}_x \psi_e \qquad 2.3.2$$

where ψ_e and ψ_m are solutions of the scalar wave equation

$$[\nabla^2 + k^2]\ \psi = 0. \qquad 2.3.3$$

A linear superposition of plane wave solutions apropos to this problem (See Figure 2.1) is, for Region (1)

$$\psi_m = \frac{1}{(2\pi)^2} \int_{-\infty}^{\infty}\int (f_1^+ e^{jW_1 z} + f_1^- e^{-jW_1 z}) e^{j(ux + vy)} dudv \qquad 2.3.4$$

$$\psi_e = \frac{1}{(2\pi)^2} \int_{-\infty}^{\infty}\int (g_1^+ e^{jW_1 z} + g_1^- e^{-jW_1 z}) e^{j(ux + vy)} dudv \qquad 2.3.5$$

And for Region (2)

$$\psi_m = \frac{1}{(2\pi)^2} \int_{-\infty}^{\infty}\int f_2(u, v)\ e^{j(ux + vy)} e^{jW_2 z}\ dudv \qquad 2.3.6$$

$$\psi_e = \frac{1}{(2\pi)^2} \int_{-\infty}^{\infty}\int g_2(u, v)\ e^{j(ux + vy)} e^{jW_2 z}\ dudv \qquad 2.3.7$$

where

$$W = \sqrt{k^{*2} - u^2 - v^2} \qquad 2.3.8$$

$$k^* = 2\pi f \sqrt{\mu \epsilon^*}\ . \qquad 2.3.9$$

From Maxwell's equations

$$\bar{E} = \frac{1}{j\omega\epsilon} \nabla x \nabla x\ \bar{A} - \nabla x\ \bar{F} \qquad 2.3.10$$

$$\bar{H} = \frac{1}{j\omega\mu} \nabla x \nabla x\ \bar{F} + \nabla x\ \bar{A}. \qquad 2.3.11$$

Making the appropriate substitutions and carrying out the indicated operations yields the following equations for the electric fields (See Figure 2.1). Region (1)

$$E_{fx} = \frac{1}{(2\pi)^2} \int\int_{-\infty}^{\infty} \frac{W_1^2 + v^2}{j\omega\epsilon_1} (f_1^+ e^{jW_1 z} + f_1^- e^{-jW_1 z}) e^{j(ux+vy)} dudv \quad 2.3.12$$

$$E_{fy} = \frac{1}{(2\pi)^2} \int\int_{-\infty}^{\infty} \frac{-uv}{j\omega\epsilon_1} [(f_1^+ e^{jW_1 z} + f_1^- e^{-jW_1 z}) - jW_1 (g_1^+ e^{jW_1 z} - g_1^- e^{-jW_1 z})] e^{j(ux + vy)} dudv \quad 2.3.13$$

$$E_{fz} = \frac{1}{(2\pi)^2} \int\int_{-\infty}^{\infty} \frac{-uW_1}{j\omega\epsilon_1} [(f_1^+ e^{jW_1 z} - f_1^- e^{-jW_1 z}) - jv(g_1^+ e^{jW_1 z} + g_1^- e^{-jW_1 z}] e^{j(ux + vy)} dudv \quad 2.3.14$$

Region (2)

$$E_{mx} = \frac{1}{(2\pi)^2} \int\int_{-\infty}^{\infty} \frac{W_2^2 + v^2}{j\omega\epsilon_2} f_2 e^{jW_2 z} e^{j(ux + vy)} dudv \quad 2.3.15$$

$$E_{my} = \frac{1}{(2\pi)^2} \int\int_{-\infty}^{\infty} (\frac{-uv}{j\omega_2} f_2 - j W_2 g_2) e^{jW_2 z} e^{j(ux + vy)} dudv \quad 2.3.16$$

$$E_{mz} = \frac{1}{(2\pi)^2} \int\int_{-\infty}^{\infty} (\frac{-uW_2}{j\omega_2} f_2 + j g_2) e^{jW_2 z} e^{j(ux + vy)} dudv \quad 2.3.17$$

Matching boundary conditions at $z = 0$ and $z = z_1$ and solving the six resulting simultaneous equations gives the various f's and g's. This has been done by Guy[13] with the following results for the fat-muscle case under investigation.

Region (1), in the fat

$$E_{fx} = \int_{-\infty}^{\infty}\int \psi_1(u, v, z)\, e^{j(ux + vy)}dudv \qquad 2.3.18$$

$$E_{fy} = \int_{-\infty}^{\infty}\int \phi_1(u, v, z)\, e^{j(ux + vy)}dudv \qquad 2.3.19$$

$$E_{fz} = \int_{-\infty}^{\infty}\int \chi_1(u, v, z)\, e^{j(ux + vy)}\, dudv \qquad 2.3.20$$

Region (2), in the muscle

$$E_{mx} = \int_{-\infty}^{\infty}\int \psi_2(u, v, z)\, e^{j(ux + vy)}\, dudv \qquad 2.3.21$$

$$E_{my} = \int_{-\infty}^{\infty}\int \phi_2(u, v, z)\, e^{j(ux + vy)}\, dudv \qquad 2.3.22$$

$$E_{mz} = \int_{-\infty}^{\infty}\int \chi_2(u, v, z)\, e^{j(ux + vy)}\, dudv \qquad 2.3.23$$

where

$$\psi_1(u, v, z) = \frac{F^-(u, v, z)}{F^-(u, v, 0)}\ \xi \qquad 2.3.24$$

$$\phi_1(u, v, z) = \frac{-uv\,\xi}{(W_1^2 + v^2)F^-(u, v, 0)} [F^-(u, v, z) - G^-(u, v, z)] \qquad 2.3.25$$

$$\chi_1(u, v, z) = \frac{-uv\,\xi}{(W_1^2 + v^2)F^-(u, v, 0)} [\frac{W_1}{v} F^+(u, v, z) + \frac{v}{W_1} G^+(u, v, z)] \qquad 2.3.26$$

$$\psi_2(u, v, z) = \frac{F^-(u, v, z_1)}{F^-(u, v, 0)} \xi\, e^{jW_2(z - z_1)} \qquad 2.3.27$$

$$\phi_2(u, v, z) = \frac{-uv e^{jW_2(z - z_1)} \xi}{(W_2^2 + v^2)F^-(u, v, 0)} [F^-(u, v, z_1) + G^+(u, v, z_1)] \qquad 2.3.28$$

$$\chi_2(u, v, z) = \frac{-uv e^{jW_2(z - z_1)} \xi}{(W_2^2 + v^2)F^-(u, v, 0)} [\frac{W_2}{v} F^-(u, v, z_1) + \frac{v}{W_1} G^+(u, v, z_1)]. \qquad 2.3.29$$

The F's and G's are given by

$$F^{\pm}(u, v, z) = (A^+ \sin W_1 z_1 + j B^+ \cos W_1 z_1) e^{jW_1(z - z_1)}$$

$$\pm(A^- \sin W_1 z_1 + j B^- \cos W_1 z_1) e^{-jW_1(z - z_1)} \qquad 2.3.30$$

$$G^{\pm}(u, v, z) = [(A^+ + B^+)\sin W_1 z_1 + jC^+ e^{jW_1 z_1}] e^{jW_1(z - z_1)}$$

$$\pm[(A^- - B^-)\sin W_1 z_1 - jC^- e^{-jW_1 z_1}] e^{-jW_1(z - z_1)}, \qquad 2.3.21$$

where

$$A^{\pm} = W_1 W_2 k^2 \epsilon_2^* \mp u^2 v^2 \pm (W_1^2 + u^2)(W_2^2 + v^2) \qquad 2.3.32$$

$$B^{\pm} = (W_1^2 + v^2)(W_2^2 + u^2) - u^2 v^2 \pm W_1 W_2 k^2 \epsilon_1^* \qquad 2.3.33$$

$$C^{\pm} = W_1 W_2 k^2 \epsilon_1^* \pm W_1^2 k^2 \epsilon_1^* . \qquad 2.3.34$$

Since the source field is at $z = 0$, then for all $z > 0$ the fields must represent waves travelling and attenuating in the z-direction. That is, the branches of the propagation constants W_1 and W_2 must be chosen to yield these characteristics. Such a choice is

$$W_1 = -\sqrt{k^2 \epsilon_1^* - u^2 - v^2} \qquad 0 < u^2 + v^2 \leq \mathrm{Re}(k^2 \epsilon_1^*) \qquad 2.3.35$$

$$W_1 = j\sqrt{u^2 + v^2 - k^2 \epsilon_1^*} \qquad \mathrm{Re}(k^2 \epsilon_1^*) \leq u^2 v^2 , \qquad 2.3.36$$

$$W_2 = -\sqrt{k^2 \epsilon_2^* - u^2 - v^2} \qquad 0 \leq u^2 + v^2 \leq \mathrm{Re}(k^2 \epsilon_2^*) \qquad 2.3.37$$

$$W_2 = j\sqrt{u^2 + v^2 - k^2 \epsilon_2^*} , \qquad \mathrm{Re}(k^2 \epsilon_2^*) \leq u^2 + v^2 \qquad 2.3.38$$

where

$$\epsilon_1^* = \epsilon_1 (1 - j\tau_1) \qquad 2.3.39$$

$$\epsilon_2^* = \epsilon_2 (1 - j\tau_2) \qquad 2.3.40$$

$$k = \frac{2\pi f}{c} . \qquad 2.3.41$$

Now, the ξ which appears in each of the electric field equations is the Fourier transform of the electric fields at aperture, i.e., $z = 0^-$.

2.4 Electric Fields in Single Semi-infinite Layer

When only a single semi-infinite muscle layer is considered, the equations in the previous section can be completely utilized by setting

z_1 equal to some convenient value such as one (1) centimeter for normalization purposes and by letting $W_1 = W_2$, $\epsilon_1^* = \epsilon_2^*$.

Another method of obtaining the expressions for a single layer medium is to utilize the equations for region (2) and match boundary conditions at $z = 0$. Both methods are easy to carry out, and since the results are relatively simple, they will not be included in this discussion.

2.5 The Theoretical Problem

An independent choice of any two of the field quantities will automatically determine all other field quantities.[12] For purposes of this research, the field quantities will be chosen to describe a field configuration at the aperture which is that corresponding to a TE_{10} waveguide mode.

The electric field in the x-direction is chosen to be of a uniform magnitude and phase along the x-direction and a cosine magnitude variation with constant phase in the y-direction. The electric field in the y-direction is zero everywhere in the aperture.

This can be mathematically stated as

$$E_x(x, y, 0) = 0 \qquad -\infty \leq y < -\frac{b}{2};\ \frac{b}{2} < y \qquad 2.5.1$$

$$E_x(x, y, 0) = \text{Cos}\,\frac{\pi y}{a} \qquad -\frac{b}{2} \leq y \leq \frac{b}{2} \qquad 2.5.2$$

$$E_y(x, y, 0) = 0 \qquad -\infty \leq x \leq \infty \qquad 2.5.3$$

2.6 Errors Due to Less Than Infinite Integration

A completely accurate computation of the electric fields at any point (x, y, z) would necessitate integration over the complete infinite $u - v$ plane. Such an analysis in this problem is entirely unrealistic and would usually make only extremely insignificant contributions outside the normal, finite ranges of integration.

Occasionally, for some integration methods, significant computational errors will result when the integration is carried out over finite limits. For the problem defined in the previous section, two specific instances exist for which finite integration fails to yield answers which are devoid of significant computational errors.

First, when electric fields exist near a conducting wedge (See Figure 2.2), a phenomenon known as edge effect arises. Near a conduction wedge, some field quantities will tend toward infinity as the edge is approached even though the energy remains finite. This edge effect will produce very high field strengths near the edges of the aperture and hot spots in the relative heating pattern.

In the analysis of the edge effect, Guy[13] assumed a single homogeneous semi-infinite lossy medium. This assumption does not account for reflections from the fat-muscle interface, and when z_1, the distance from the surface to the fat-muscle interface, is small, this assumption introduces another error which must be corrected.

Guy[13] has analyzed the two problem situations described above and derived corrections which are added to E_x and E_z when x and z are

in close proximity to the aperture edge or when z_1 is so small that imaging effects must be taken into account. The corrections are given by

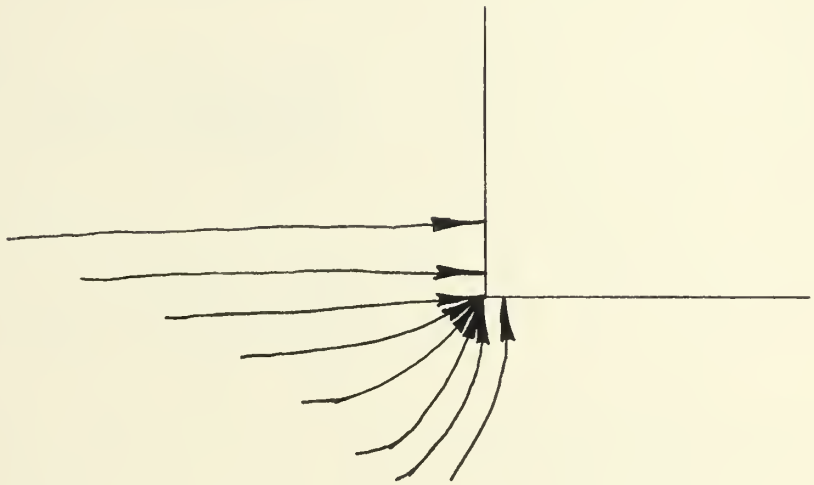

Figure 2.2

The Edge Effect

$$C_x = \cos\left(\frac{\pi y}{a}\right)\left[-\int_{-U_{max}}^{U_{max}} \frac{\sin\left(\frac{bu}{2}\right)}{\left(\frac{bu}{2}\right)} e^{jux} e^{-uz}\, du \right.$$

$$+ \tan^{-1}\frac{\left(\frac{b}{2} + x\right)}{z} + \tan^{-1}\frac{\left(\frac{b}{2} - x\right)}{z}$$

$$\left. - \tan^{-1}\frac{\left(\frac{b}{2} + x\right)}{(z + z_1)} - \tan^{-1}\frac{\left(\frac{b}{2} - x\right)}{(z + z_1)} \right] \qquad 2.6.1$$

$$C_z = \cos\left(\frac{y}{a}\right)\left[-\int_{-U_{max}}^{U_{max}} \frac{\sin\left(\frac{bu}{2}\right)}{\left(\frac{bu}{2}\right)} e^{jux} e^{-uz}\, du \right.$$

$$+ \tfrac{1}{2} \ell n \frac{z^2 + \left(\frac{b}{2} + x\right)^2}{z^2 + \left(\frac{b}{2} - x\right)^2}$$

$$\left. + \ell n \frac{(z + z_1)^2 + \left(\frac{b}{2} + x\right)^2}{(z + z_1)^2 + \left(\frac{b}{2} - x\right)^2} \right] \qquad 2.6.2$$

These corrections are to be added to the electric fields at points near the edge of the aperture and at all points in the Region (1) expressions for E_x and E_y when z_1 is small enough to cause imaging. Note that the integrands in the correction can be subtracted from the integrands derived in Section 2.3 before the integration with respect to u is performed.

All of the necessary equations for computing relative heating patterns have now been developed. Attention can now be focused on an efficient algorithm to compute the necessary transformations.

CHAPTER 3

THE FAST FOURIER TRANSFORM

3.1 Background

Since 1822 when Jean Baptiste Fourier (1768-1830) published his Theorie Analytique de la Chaleur, in which he set forth the trigonometric series and integrals which are named after him, Fourier analysis has played an important role in the analysis of many of the problems of physics and engineering. Fourier himself only presented the general boundary value problem for the case of heat conduction, but today his methods find wide application in the disciplines metnioned above. Besides the heat conduction problem where the method is still apropos, many problems of today are particularly amendable to the method; to name a few:

a. Power spectral density

b. System simulation

c. Noise analysis

d. Statistical distribution analysis

e. Frequency analysis of bandlimited waveforms

f. Convolution (lagged product) problems

g. Acoustic wave propogation

h. Speech transmission

i. Transport phenomena

j. Optics

k. Electro magnetics.

3.2 Fourier Analysis

The theory of Fourier analysis is beyond the scope of this report,[14, 15] but several excellent texts exist pertaining to this subject.

The major drawback of Fourier analysis lies in the need to evaluate integrals which have infinite limits, as is seen in the one-dimensional Fourier transform pair utilized in frequency analysis:

$$S(f) = \frac{1}{\sqrt{2\pi}} \int_{-\infty}^{\infty} x(t)\, e^{-j2\pi ft}\, dt \qquad 3.2.1$$

$$x(t) = \frac{1}{\sqrt{2\pi}} \int_{-\infty}^{\infty} s(f)\, e^{j2\pi ft}\, df \qquad 3.2.2$$

or the equivalent two-dimensional form usually seen in boundary value problems:

$$S(u, v) = \frac{1}{2\pi} \int\int_{-\infty}^{\infty} d(x, y)\, e^{-j(ux + vy)}\, dxdy \qquad 3.2.3$$

$$d(x, y) = \frac{1}{2\pi} \int\int_{-\infty}^{\infty} S(u, v)\, e^{j(ux + vy)}\, dudv \qquad 3.2.4$$

Equations 3.2.3 and 3.2.4 are typical of those developed in Chapter 2, but for purposes of illustration of the FFT the equations 3.2.1 and 3.2.2 will be used.

3.3 The Fast Fourier Transform

Prior to the advent of high speed computers, complex integration was handled by such methods as the saddle point or stationary phase

techniques which are valid only for expressions of large argument. Thus the really important questions of analysis of near zone fields of an antenna were seldom investigated since in this area the integrals were unassailable by analytic methods, except in a few special cases. The computer changed this, but did not significantly advance the state of the art due to the high cost of computing time.

A real advance came when Cooley and Tukey[16] found the algorithm known as the fast Fourier transform. It then became economical to compute discrete Fourier transforms, and many problems could be economically investigated.

Returning now to the Fourier transform itself, and in particular looking at the discrete Fourier transform pair associated with equations 3.2.1 and 3.2.2,

$$S(f_n) = \Delta t \sum_{k=0}^{N-1} x(t_k)\, e^{-j2\pi f_n t_k} \qquad n = 0, \pm 1, \pm 2, \ldots \pm\frac{N}{2} \qquad 3.3.1$$

$$x(t_k) = \Delta f \sum_{n=N/2}^{N/2} S(f_n)\, e^{j2\pi f_n t_k} \qquad k = 0, +1, +2, \ldots N-1 \qquad 3.3.2$$

now, making the following substitutions,

$$t_k = k\Delta t \qquad t = T/N$$

$$f_n = n\Delta f \qquad f = \frac{1}{T}$$

then equations 3.3.1 and 3.3.2 become, according to Cooley,[17]

$$S(n) = \sum_{k=0}^{N-1} x(k)\, e^{-j2\pi (nk)/N} \qquad 3.3.3$$

$$n = 0, +1, +2, \ldots N-1$$

$$k = 0, +1, +2, \ldots N-1$$

$$x(k) = \sum_{n=0}^{N-1} S(n)\, e^{j2\pi (nk)/N} \; . \qquad 3.3.4$$

3.4 Factoring the Transform

For purposes of illustration, when equation 3.3.3 is written out in full for $N = 4$ and with $W^{\ell} = e^{-j2\pi\ell/N}$, Brigham and Morrow[18] define

$$[S(n)] = \begin{bmatrix} W^0 & W^0 & W^0 & W^0 \\ W^0 & W^1 & W^2 & W^3 \\ W^0 & W^2 & W^4 & W^6 \\ W^0 & W^3 & W^6 & W^9 \end{bmatrix} \begin{bmatrix} x_0(0) \\ x_0(1) \\ x_0(2) \\ x_0(3) \end{bmatrix} = \begin{matrix} S(0) \\ S(1) \\ S(2) \\ S(3) \end{matrix} \; . \qquad 3.4.1$$

Now define $\overline{[S(n)]}$ as:

$$[\overline{S(n)}] = \begin{bmatrix} S(0) \\ S(2) \\ S(1) \\ S(3) \end{bmatrix} = \begin{bmatrix} W^0 & W^0 & W^0 & W^0 \\ W^0 & W^2 & W^4 & W^6 \\ W^0 & W^1 & W^2 & W^3 \\ W^0 & W^3 & W^6 & W^9 \end{bmatrix} \begin{bmatrix} x_0(0) \\ x_0(1) \\ x_0(2) \\ x_0(3) \end{bmatrix} = [W][x_0(n)] \qquad 3.4.2$$

The $[W]$ matrix in 3.4.2 can now be factored, and since $W^0 = 1$

$$\overline{[S(n)]} = \begin{bmatrix} 1 & W^0 & 0 & 0 \\ 1 & W^2 & 0 & 0 \\ 0 & 0 & 1 & W^1 \\ 0 & 0 & 1 & W^3 \end{bmatrix} \begin{bmatrix} 1 & 1 & W^0 & 0 \\ 0 & 1 & 0 & W^0 \\ 1 & 0 & W^2 & 0 \\ 0 & 1 & 0 & W^2 \end{bmatrix} \begin{bmatrix} x_0(0) \\ x_0(1) \\ x_0(2) \\ x_0(3) \end{bmatrix} \qquad 3.4.3$$

Alternately, this can be written:

$$\overline{[S(n)]} = [x_2(n)] = \begin{bmatrix} 1 & W^0 & 0 & 0 \\ 1 & W^2 & 0 & 0 \\ 0 & 0 & 1 & W^1 \\ 0 & 0 & 1 & W^3 \end{bmatrix} [x_1(n)] \qquad 3.4.4$$

where:

$$[x_1(n)] = \begin{bmatrix} 1 & 0 & W^0 & 0 \\ 0 & 1 & 0 & W^0 \\ 1 & 0 & W^2 & 0 \\ 0 & 1 & 0 & W^2 \end{bmatrix} [x_0(n)] \qquad 3.4.5$$

This factorization looks somewhat mystical, so to put minds at ease and insure that the factorization is valid, and to insure that equation 3.4.4 agrees with 3.3.3, from equation 3.4.4,

$$\overline{[S(n)]} = \begin{bmatrix} x_1(0) + x_1(1)W^0 \\ x_1(0) + x_1(1)W^2 \\ x_1(2) + x_1(3)W^1 \\ x_1(2) + x_1(3)W^3 \end{bmatrix} ; \qquad 3.4.6$$

and from equation 3.4.5,

$$[x_1(n)] = \begin{bmatrix} x_0(0) + x_0(2)W^0 \\ x_0(1) + x_0(3)W^0 \\ x_0(0) + x_0(2)W^2 \\ x_0(1) + x_0(3)W^2 \end{bmatrix} ; \qquad 3.4.7$$

then, substituting 3.4.7 into 3.4.6 yields

$$\overline{[S(n)]} = \begin{bmatrix} x_0(0) + x_0(2)W^0 + (x_0(1) + x_0(3)W^0)W^0 \\ x_0(0) + x_0(2)W^0 + (x_0(1) + x_0(3)W^0)W^2 \\ x_0(0) + x_0(2)W^2 + (x_0(1) + x_0(3)W^2)W^1 \\ x_0(0) + x_0(2)W^2 + (x_0(1) + x_0(3)W^2)W^3 \end{bmatrix} . \qquad 3.4.8$$

If we note that $W^n = W^{n\pm4}$ or, more generally speaking $W^n = W^{n\pm4k}$, where k is some integer, then 3.4.8 upon rearrangement becomes once again equation 3.4.2 written out in full, instead of matrix form:

$$\overline{[S(n)]} = \begin{bmatrix} x_0(0) + x_0(1)W^0 + x_0(2)W^0 + x_0(3)W^0 \\ x_0(0) + x_0(1)W^2 + x_0(2)W^4 + x_0(3)W^6 \\ x_0(0) + x_0(1)W^1 + x_0(2)W^2 + x_0(3)W^3 \\ x_0(0) + x_0(1)W^3 + x_0(2)W^6 + x_0(3)W^9 \end{bmatrix} . \qquad 3.4.9$$

One discrepancy has arisen in that we have derived $[\overline{S(n)}]$ instead of $S(n)$. This can very easily be corrected by an algorithm which looks at n as a binary address of a particular element of the matrix S. To find the correct address is simply a matter of bit reversing the binary number n.

Then,

$$[S(n)] = \begin{bmatrix} S(00) \\ S(01) \\ S(10) \\ S(11) \end{bmatrix} \qquad 3.4.10$$

and bit reversing the address yields

$$\overline{[S(n)]} = \begin{bmatrix} S(00) \\ S(10) \\ S(01) \\ S(11) \end{bmatrix} . \qquad 3.4.11$$

While it is true that the above development applies only to the case $N = 4$ and not to the general case, when the discrete Fourier transform, equation 3.3.3, is examined for a general case, as has been shown by Gentleman and Sande, [19] then the factorization can be performed for any N that is not a prime number. This factorization is a recursive formula which defines larger Fourier transforms in terms of smaller transforms. A multi-dimensional discrete Fourier transform, such as this research investigates, can be efficiently computed by performing the factorization in each dimension separately.

3.5 The Algorithm

The obvious question to ask now, is how to obtain the factored matrices indicated in equation 3.4.3. This is most easily seen in a

tree graph (See Figures 3.1 and 3.2) where a vertical column of nodes will correspond to the $x_\ell(k)$ arrays (where for our example $\ell = 0, 1, 2$). For cases where $N = 2^\gamma$(γ an integer), we will have $\gamma + 1$ vertical arrays and N horizontal arrays. For this example we will use $\gamma = 2$, $N = 2^2 = 4$. In the tree graph, a solid line will indicate that the node in the previous vertical array is to be multiplied by the W factor raised to the power indicated in the node of interest, then added to the value of the node from which the dashed line originates. The following algorithm yields the necessary node integers.

1. Express the argument k as a binary number.
2. For the ℓ^{th} array, shift the number $\gamma - \ell$ places to the right and reverse the bits.

To find out where the solid and dashed lines originate:

1. Let the argument k be expressed as a binary number such that $k = k_{\gamma-1}, k_{\gamma-2}, \ldots k_0$. Thus if $k = 6$, $\gamma = 3$ then $k_2 = 1$, $k_1 = 1$, $k_0 = 0$ or $k_2k_1k_0 = 110)_2 = 6)_{10}$.
2. Now in the ℓ^{th} array, node k has a solid line from k^{th} node in the $\ell - 1$ array except that $k_{\gamma-\ell}$ is a one (1).
3. A dashed line originates from address k except that $k_{\gamma-\ell}$ is a zero (0).

To see how this works, apply the rules to two cases $N = 4$, $N = 8$ and arrive at the tree graphs shown in Figures 3.1 and 3.2 respectively.

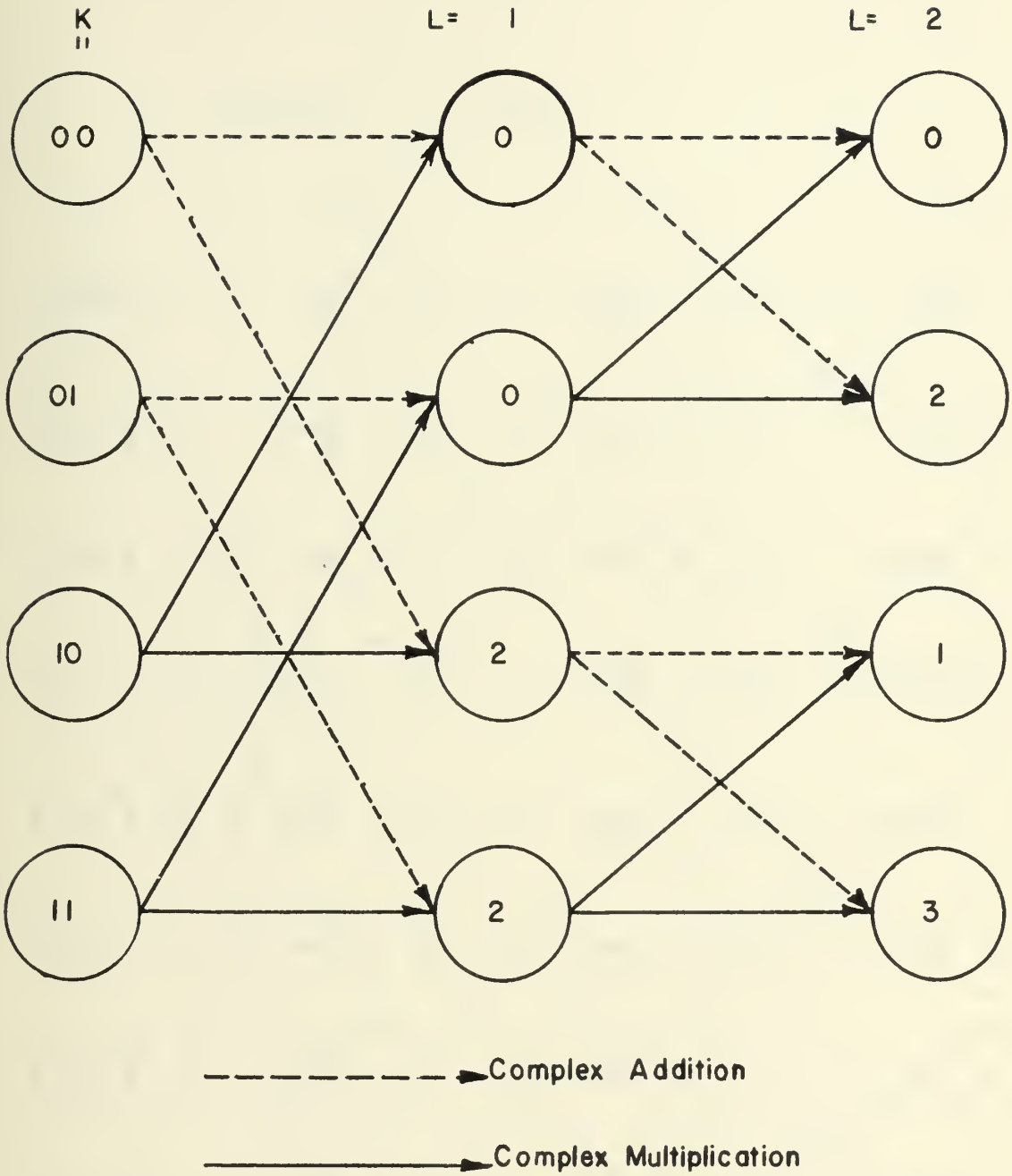

FIGURE 3. 1

Tree Graph, N = 4

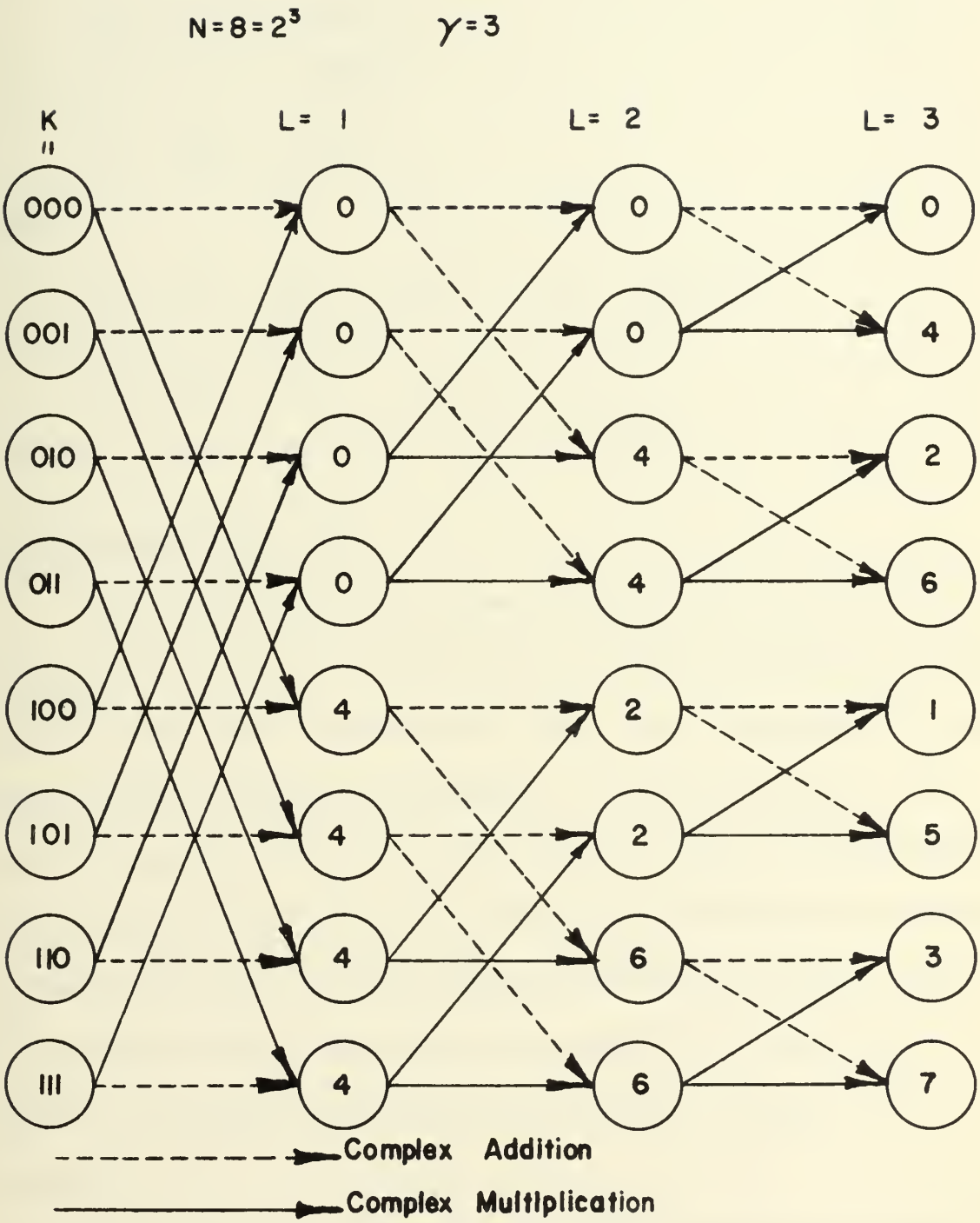

FIGURE 3.2

Tree Graph, N = 8

Now verify the tree graph by looking at $S(1) = x_2(1)$ in Figure 3.1.

$$x_2(1) = x_1(2) + x_1(3)W^1$$
$$x_1(2) = x_0(0) + x_0(2)W^2$$
$$x_1(3) = x_0(1) + x_0(3)W^2 \qquad 3.5.1$$

Then,

$$S(1) = x_2(1) = x_0(0) + x_0(2)W^2 + (x_0(1) + x_0(3)W^2)W^1$$
$$S(1) = x_0(0) + x_0(1)W^1 + x_0(2)W^2 + x_0(3)W^3, \qquad 3.5.2$$

which is in complete agreement with prior results.

3.6 Advantage of the FFT

The conventional method of performing Fourier analysis on a set of data points consists of summing a finite number of terms in a Fourier series to obtain each transformed data point. Each term added into the series requires a complex multiplication to obtain the term and a complex addition to include the term in the series. Thus, if N data points are to be transformed utilizing N terms of the series and one complex multiplication and one complex addition constitute one operation, then N^2 operations must be performed to accomplish the transformation. Likewise, a two-dimensional array of data points will require N^4 operations.

By comparison, the FFT requires N operations for each set of nodes and must have $\log_2 N$ sets of nodes which results in a total of

$N\log_2 N$ operations for a one-dimensional transform. For the two-dimensional case $4N^2\log_2 N$ operations are required.

With the above results, the time savings factor (TSF) for a two-dimensional array of 64 x 64 points is

$$TSF = \frac{4N^2\log_2 N}{N^4} = \frac{4\log_2 N}{N^2} \cong \frac{1}{170} \quad . \qquad 3.6.1$$

3.7 Problems in FFT Analysis

Aliasing, leakage and the "picket fence" effect are the most common errors encountered in utilization of the fast Fourier transform.[20] The effects of these errors can usually be completely eradicated, or at the very least be reduced to acceptable levels, by insuring that the data is sampled at least twice during each cycle and by proper selection of data window.

3.8 Space and Frequency Relationships

A problem encountered in performing either the Fourier transform or the inverse Fourier transform is the correlation of a sampling rate in the frequency domain to data point incrementation in the time or special domain. In conventional Fourier analysis, the problem is resolved by the very nature of the series, in that the argument of the functions in each term of the Fourier series contains time and frequency explicitly as seen in equation 3.8.1.

$$x(t) = \sum_{n=-\infty}^{\infty} C_n e^{j2\pi n\Delta f t} . \qquad \Delta f = \frac{1}{T} \qquad 3.8.1$$

The Fourier series does not demand the computation of x at any particular t. The only requirement is that t lie within the data window $-T/2 \leq t \leq T/2$ in the asymmetric case and within $0 \leq t \leq T$ in the symmetric case when only N terms of the series are utilized.

By contrast, time and frequency are nowhere to be found in the formulation of the fast Fourier transform. This can lead to confusion and uncertainty regarding the exact coordinates of a point in either domain unless careful attention is paid to equation 3.8.2.

$$t = \frac{1}{N\Delta f} = \frac{2\pi}{N\Delta\omega} \qquad 3.8.2$$

These relations are simple, but can mislead the user of the FFT.

In order to clear up the question surrounding this problem, consider a one-dimensional problem in which an array of data points are to be (1) transformed into the frequency domain; (2) multiplied by some other function; (3) then the product transformed back into the time domain. The problem may be stated as

$$S(k) = \sum_{n=0}^{N-1} x_0(n) e^{-j2\pi nk/N} \qquad 3.8.3$$

$$x_1(n) = \frac{1}{N} \sum_{k=0}^{N-1} S(k)G(k) \; e^{j2\pi nk/N} \qquad 3.8.4$$

with the following definitions (See Figure 3.3).

T = width of data window

N = number od data points 3.8.5

These independent choices dictate the following relations.

$$\Delta x_0 = \frac{T}{N-1}$$

$$\Delta\omega = \frac{2\pi (N-1)}{NT}$$

$$F = \text{Spectral window} = \frac{N-1}{NT}$$

$$\Delta x_1 = \frac{T}{N-1} \qquad 3.8.6$$

Then, assuming G is a continuous function, it must be evaluated in the interval $-F/2 = \omega = F/2$ at N points spaced equally in increments of $\Delta\omega$. This also assumes that G is a function of ω rather than f, and this is quite often the case, e.g., the relative heating equations in the previous chapter which have been programmed utilizing the FFT and the results compared with a Gaussian quadrature transformation in the next chapter.

CHAPTER 4

UTILITZATION OF THE FFT ON RELATIVE HEATING PROBLEMS

4.1 Introduction

Diathermy, the therapeutic heating of deep body tissue, is an important part of physical medicine and rehabilitation. Research at the University of Washington in this field is concerned with the determination of an optimum frequency and aperture configuration which will yield good heating in musculature without excess heating in the subcutaneous fat. This can be recognized in a relative heating pattern which shows low heating in the fat relative to the amount of heating observed in the muscle.

The research basically has two phases. The first stage is a theoretical analysis of the problem utilizing plastic models of tissue and computer models of the electromagnetics. The second phase is the building and testing of diathermy applicators, once again using the already proven plastic and computer models.

Chapters 2 and 3 have laid the groundwork for a computer model of the diathermy problem. The succeeding sections of this chapter will finish the construction of the computer model. Each phase of the research has a similar, but different computer model and each will be discussed separately.

4.2 The Theoretical Phase

The first phase computer model for diathermy research consists of an executable computer algorithm which can evaluate the relative heating expressions of Chapter 2 for a theoretical aperture distribution. A suitable algorithm which can accomplish the transformations is the fast Fourier transform.

Several versions of the fast Fourier transform can be found in the literature,[21, 22] some of which are written in Fortran and others are written in Algol. The algorithm of Eguchi[21] has been used in this research for two reasons;

a.) its language is Fortran,

b.) it can be implemented on the University of Washington computers without extensive revision.

Some revision of Eguchi's program has been made to cut out the portions of his program which are not necessary in the diathermy problem. Since extensive calculations must be done to build the arrays to be transformed and the amount of memory used is a determining factor in computer costs, features in Eguchi's program such as magnitude distributions, convolutions, gradients and the various output options are unusable and have been discarded since they obligate memory that can be more efficiently used.

Figure 4.1 gives a flow chart for the use of the various subroutines given in the Appendices and outlines the method of computer solutions necessary in the first phase of diathermy research.

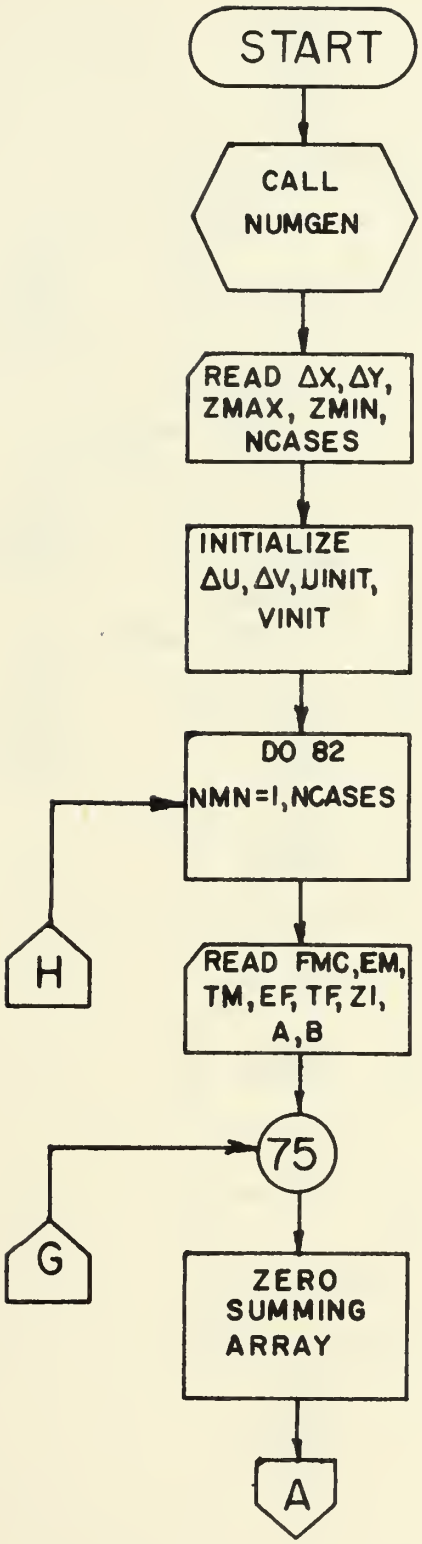

FIGURE 4. 1

Flow Chart of Theoretical Problem

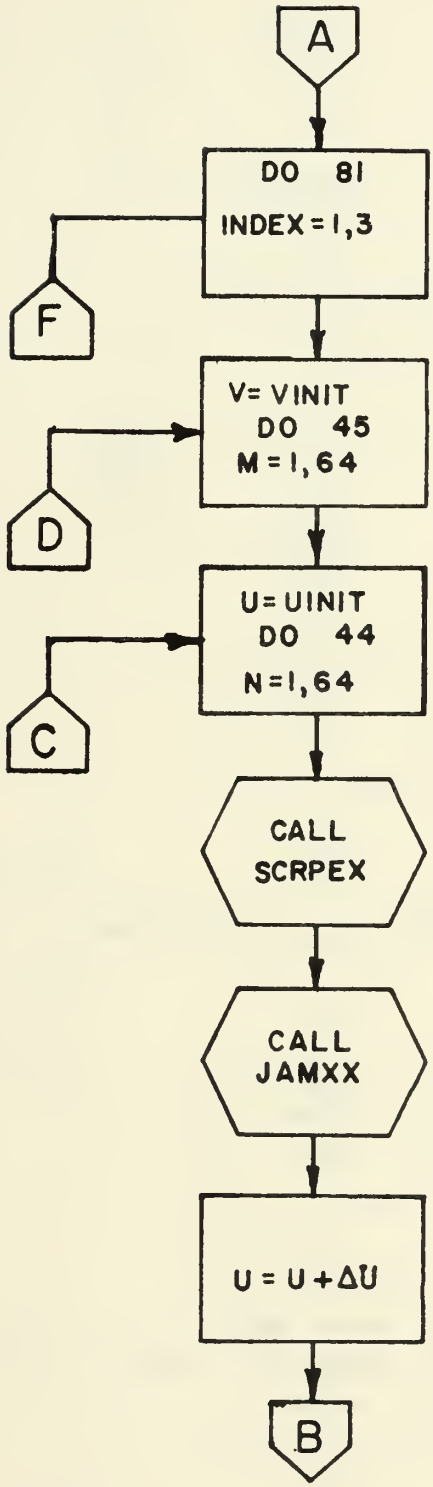

FIGURE 4. 1 (continued)

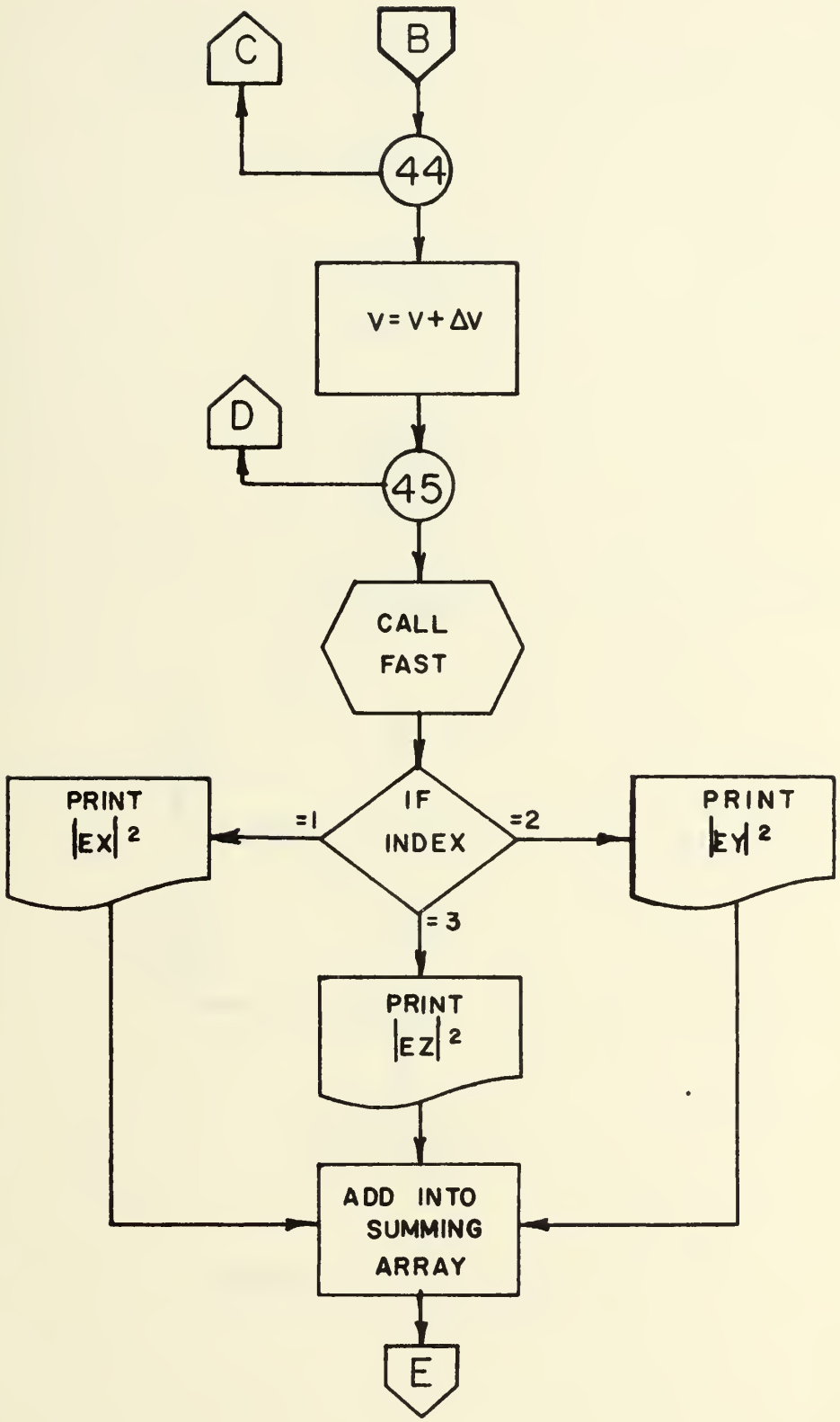

FIGURE 4. 1 (continued)

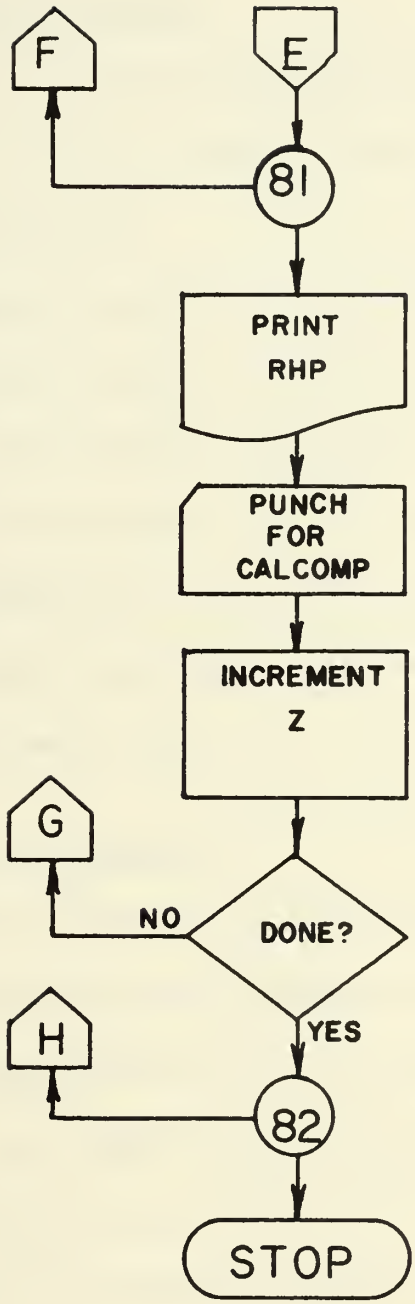

FIGURE 4. 1 (continued)

4.3 The Empirical Phase

Upon successful determination of an optimum frequency and aperture configuration, extensive tests must be made of any prototype diathermy applicators.

Utilizing the methods of the first phase computer solution and having available a sufficient amount of empirical data from the field configuation at the surface of the plastic models, the fast Fourier transform can once again be used to determine the relative heating patterns throughout the volume of the planar model.

A suitable method of solution for problems of an empirical nature is outlined in Figure 4.2.

4.4 Objective Restatement

This research is primarily concerned with evaluating the relative merits of the fast Fourier transform to the solution of the theoretical relative heating problem versus the Gaussian quadrature method currently in use. Solutions for empirical problems will follow as a direct by-product of this research. The results of computations by both methods are compared in the next chapter.

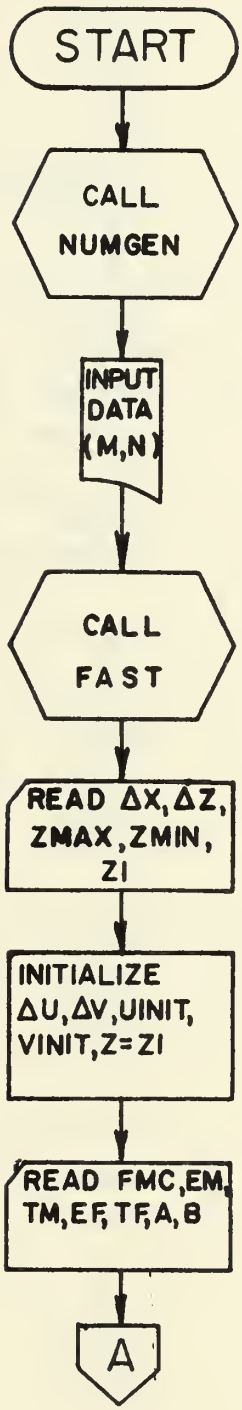

FIGURE 4.2

Flow Chart of Empirical Problem

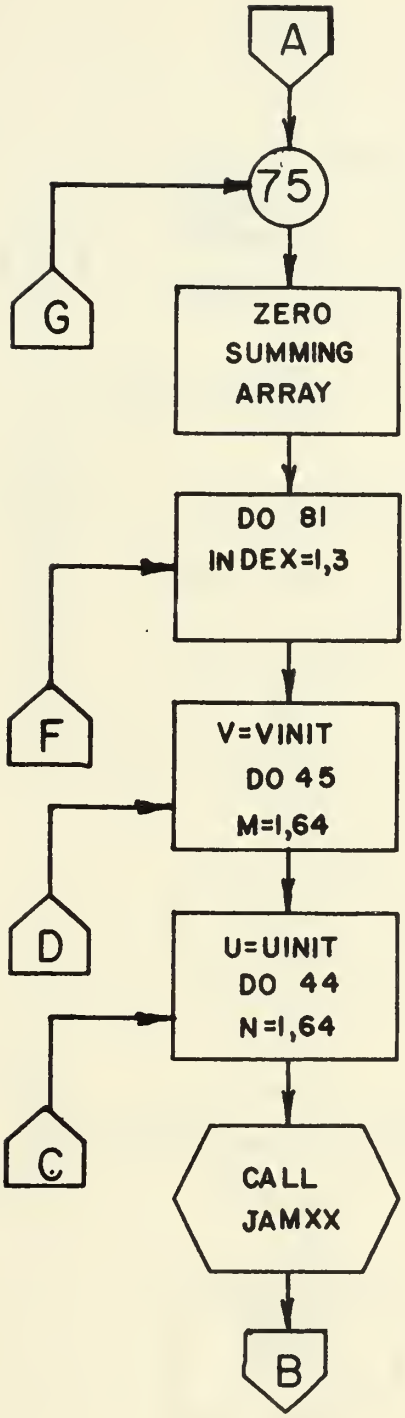

FIGURE 4. 2 (continued)

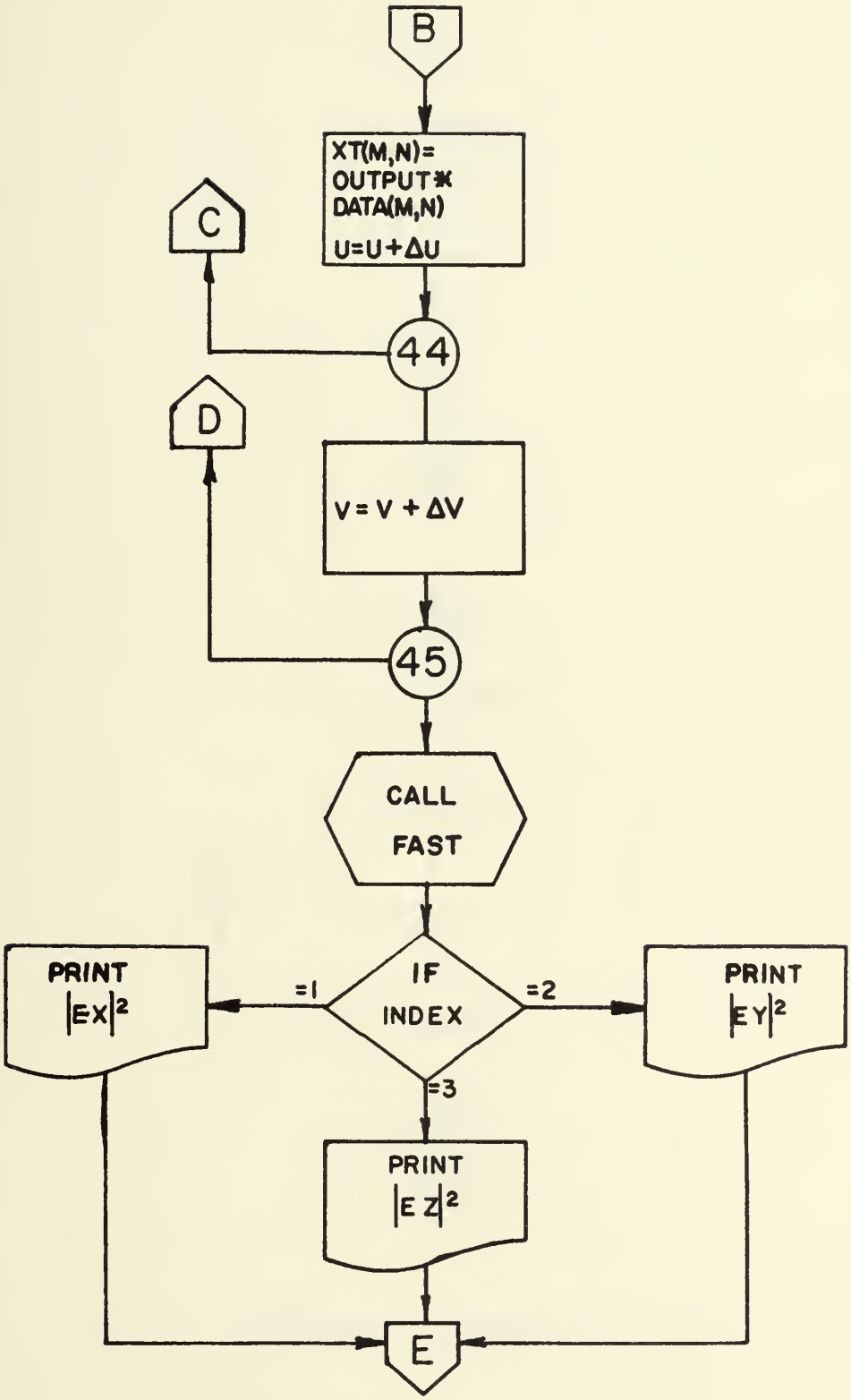

FIGURE 4. 2 (continued)

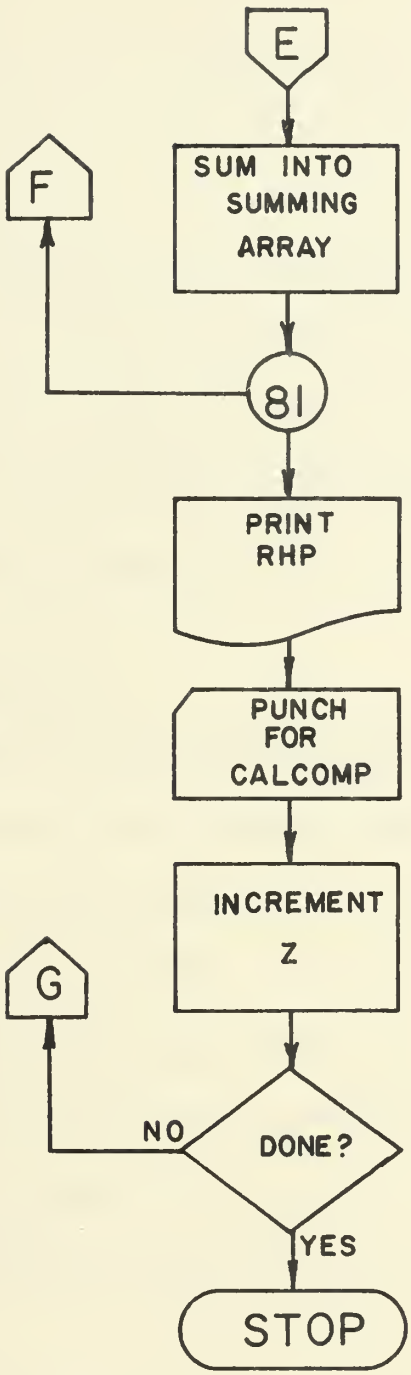

FIGURE 4.2 (continued)

CHAPTER 5

RESULTS

5.1 Introduction

Relative heating patterns (RHPS) as computed by the fast Fourier transform (FFT) and Gaussian quadrature (GQ) methods will be presented in the succeeding sections of this chapter. An error criterion will be defined and the computed relative heating values will be compared on a point by point basis whenever possible.

5.2 The Error Criterion

Any digital integration method has an associated, inherent error. Quite often, the exact error cannot be ascertained; i.e., the bounds of the error are all that can be established. At other times, even the error bounds are difficult to establish. In the case of the FFT, Gentleman and Sande[13] have proven the bounds of error due to round off, but nowhere is there a complete proof of error bounds for a fast Fourier transformation. No attempt will be made here to set error bounds. Instead, the FFT will be compared to the best available values from the Gaussian quadrature method.

Since both methods have inherent inaccuracies due to less than infinite integration, any error encountered in comparing results will also contain inaccuracies which are impossible to establish. For purposes of this research, error will be defined as the absolute difference in relative

heating values at the point (x, y, z) as computed by the Gaussian quadrature and fast Fourier transform methods. This error will be put on a percentage basis by dividing the magnitude of the error by the magnitude of the normalization point always has a value of unity in both methods, the point $(0, 0, z_1)$ will always have zero error when comparing the two transformation methods. This definition is then

$$\% \text{ ERROR} = 100 \text{ (PGAUSS - PFFT)} \qquad 5.2.1$$

where PGAUSS and PFFT are the relative heating values computed at (x, y, z) by the Gaussian quadrature and fast Fourier transformations respectively.

To be an acceptable tool for computing relative heating patterns, the fast Fourier transform must compute values to within 5% ERROR, except at points which lie along lines with very steep slopes.

5.3 Data Presentation

Relative heating values and the associated error are tabulated in Tables 5.2 - 5.6 for several different frequencies. Each table is followed by CALCOMP plots which give a visual representation of the relative heating patterns as computed by the FFT and Gaussian quadrature methods, in that order. Table 5.1 list the frequencies, associated dielectric constants, and loss tangents used in each of the five cases considered. East case considers a rectangular aperture (12 x 16cm.) in an infinite ground plane (See Figure 2.1). The relative heating

patterns were computed at $Z = 0.1, 1.0, 2.0, 3.0, 4.0$cm. with the fat muscle interface occurring in each case at $Z_1 = 2.0$cm.

A brief explanation is in order concerning the CALCOMP plots which follow each tabulated comparison of the two methods. The first plot is a relative heating pattern as computed by the FFT. This is followed immediately by a transparency taken from the FFT results. This transparency overlays a relative heating pattern for the same case as computed by the GQ method.

The transparencies unavoidably shrunk somewhat in processing, nevertheless they provide an excellent visual comparison of the two computational methods. For example, examine Figures 5.3, 5.3a, 5.4 which are the relative heating patterns for the 750 mHz comparison in Table 5.3. The following agreements and discrepancies are readily identifiable in the overlay:

a. There is very good agreement in the two plots for $Z = 1$ and 4 cm.

b. The $Z = 3$ cm. curves differ by about 1% in the range 3 cm. $\leq x \leq$ 8 cm.

c. About 2% difference can be seen in the $Z = 2$ cm. curves in the range 1 cm. $\leq x \leq$ 8 cm.

d. The FFT curve for $Z = 0.1$ cm. has some aliasing due to the truncated series, but shows good agreement with the GQ curve except at the edge of the aperture.

Similar comparisons can be made for each frequency, but will not be made here.

Table 5.1

Input Data

F	ϵ_m	τ_m	ϵ_f	τ_f
400 MHZ	52.79	0.9842	5.55	0.3745
750 MHZ	51.54	.5944	5.59	.2659
918.8 MHZ	51.4	.488	5.75	.25
1500 MHZ	49.52	.3858	5.58	.1943
2450 MHZ	47.42	0.3059	5.56	0.1541

F = frequency

ϵ_m = dielectric constant in muscle

τ_m = loss tangent in muscle

ϵ_f = dielectric constant in fat

τ_f = loss tangent in fat

Table 5.2

400 MHZ

Comparison of RHPS as Computed by FFT and GQ

$Z = 0.1$ cm $Y = 0.0$ cm $Z_1 = 2.0$ cm

X	P FFT	P GAUSS	% ERROR
0.0	0.169388	0.169952	0.056
0.5	.175147	.170537	.461
1.0	.171048	.172285	.124
1.5	.178611	.175194	.342
2.0	.175963	.179276	.331
2.5	.185448	.184532	.092
3.0	.183975	.190959	.698
3.5	.195594	.198569	0.297
4.0	.194992	.207351	1.236
4.5	.209297	.217296	0.800
5.0	.209303	.228461	1.916
5.5	.227837	.241038	1.320
6.0	.228445	.255586	2.714
6.5	.256536	.273632	1.710
7.0	.259753	.299380	3.963
7.5	.332851	.347174	1.432
8.0	.326463	.437956	11.149
8.5	.151589	.190027	3.844
9.0	.090918	.130376	3.946
9.5	.066715	.100687	3.397
10.0	0.051848	0.081288	2.944

$Z = 1.0$ cm $Y = 0.0$ cm $Z_1 = 2.0$ cm

0.0	0.091048	0.090634	0.041
0.5	.091409	.091156	.025
1.0	.092435	.092712	.028
1.5	.094167	.095286	.112
2.0	.096532	.098847	.231
2.5	.099564	.103357	.379
3.0	.103185	.108777	.559
3.5	.107442	.115069	.763
4.0	.112266	.122200	0.993
4.5	.117727	.130148	1.242
5.0	.123753	.138889	1.514
5.5	.130372	.148365	1.799
6.0	0.137287	0.158386	2.110

Table 5.2 (continued)

Z = 1.0 cm Y = 0.0 cm Z_1 = 2.0 cm

X	P FFT	P GAUSS	% ERROR
6.5	0.143945	0.168356	2.441
7.0	.148450	.176575	2.812
7.5	.146659	.178684	3.203
8.0	.132127	.167522	3.539
8.5	.107165	.143679	3.651
9.0	.083202	.118478	3.528
9.5	.065198	.097531	3.233
10.0	0.052651	0.080851	2.820

Z = 2.0 cm Y = 0.0 cm Z_1 = 2.0 cm

0.0	1.000000	1.000000	0.000
0.5	0.997064	0.996597	.047
1.0	.988276	.986425	.185
1.5	.973692	.969587	.411
2.0	.953406	.946253	0.715
2.5	.927548	.916656	1.089
3.0	.896284	.881081	1.520
3.5	.859815	.839869	1.995
4.0	.818375	.793416	2.496
4.5	.772241	.742172	3.007
5.0	.721731	.686660	3.507
5.5	.667224	.627489	3.974
6.0	.609190	.565400	4.379
6.5	.548269	.501325	4.694
7.0	.485449	.436549	4.890
7.5	.422356	.372947	4.941
8.0	.361438	.313075	4.836
8.5	.305438	.259591	4.585
9.0	.256178	.214073	4.210
9.5	.213941	.176540	3.740
10.0	0.177985	0.146014	3.197

Z = 3.0 cm Y = 0.0 cm Z_1 = 2.0 cm

0.0	0.550351	0.551602	0.125
0.5	.548625	.549611	.099
1.0	.543457	.543656	.020
1.5	.534874	.533789	.109
2.0	.522926	.520097	.283
2.5	.507689	.502710	.498
3.0	0.489268	0.481801	0.747

Table 5.2 (continued)

Z = 3.0 cm Y = 0.0 cm Z_1 = 2.0 cm

X	P FFT	P GAUSS	% ERROR
3.5	0.467811	0.457597	1.022
4.0	.443515	.430385	1.313
4.5	.416643	.400537	1.611
5.0	.387545	.368519	1.903
5.5	.356670	.334904	2.177
6.0	.324587	.300397	2.419
6.5	.291979	.265826	2.615
7.0	.259628	.232110	2.752
7.5	.228338	.200174	2.816
8.0	.198829	.170832	2.800
8.5	.171621	.144637	2.698
9.0	.146975	.121814	2.516
9.5	.124916	.102294	2.262
10.0	0.105311	0.085808	1.950

Z = 4.0 cm Y = 0.0 cm Z_1 = 2.0 cm

0.0	0.300086	0.301578	0.149
0.5	.299063	.300403	.134
1.0	.296001	.296889	.089
1.5	.290926	.291075	.015
2.0	.283882	.283025	.086
2.5	.274937	.272840	.210
3.0	.264192	.260654	.354
3.5	.251782	.246649	.513
4.0	.237889	.231057	.683
4.5	.222742	.214170	0.857
5.0	.206626	.196335	1.029
5.5	.189871	.177952	1.192
6.0	.172844	.159463	1.338
6.5	.155923	.141324	1.460
7.0	.139465	.123966	1.550
7.5	.123766	.107756	1.601
8.0	.109037	.092960	1.608
8.5	.095389	.079721	1.567
9.0	.082849	.068066	1.478
9.5	.071386	.057938	1.345
10.0	0.060946	0.049218	1.173

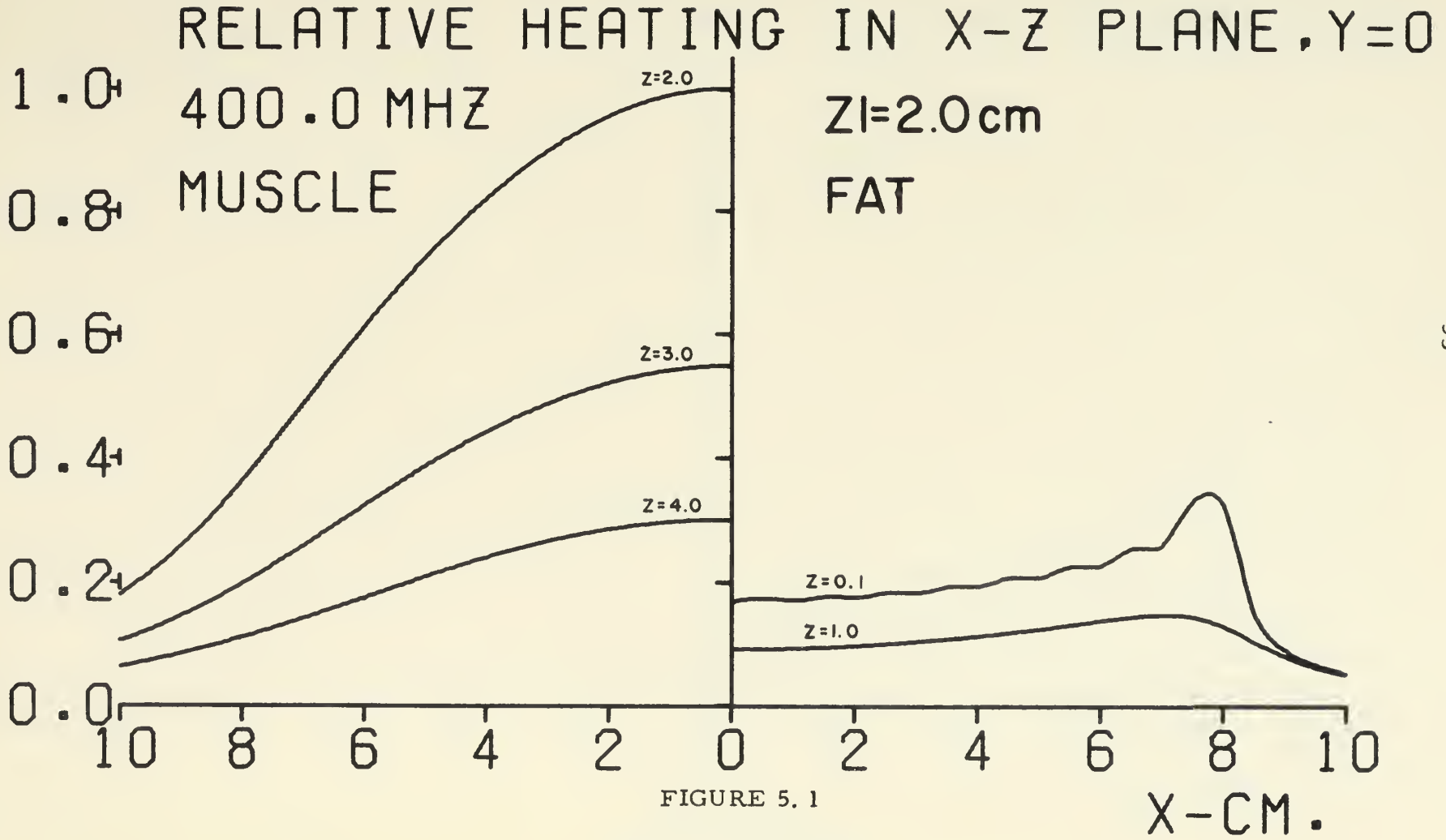

FIGURE 5.1

400 mHz FFT RHP

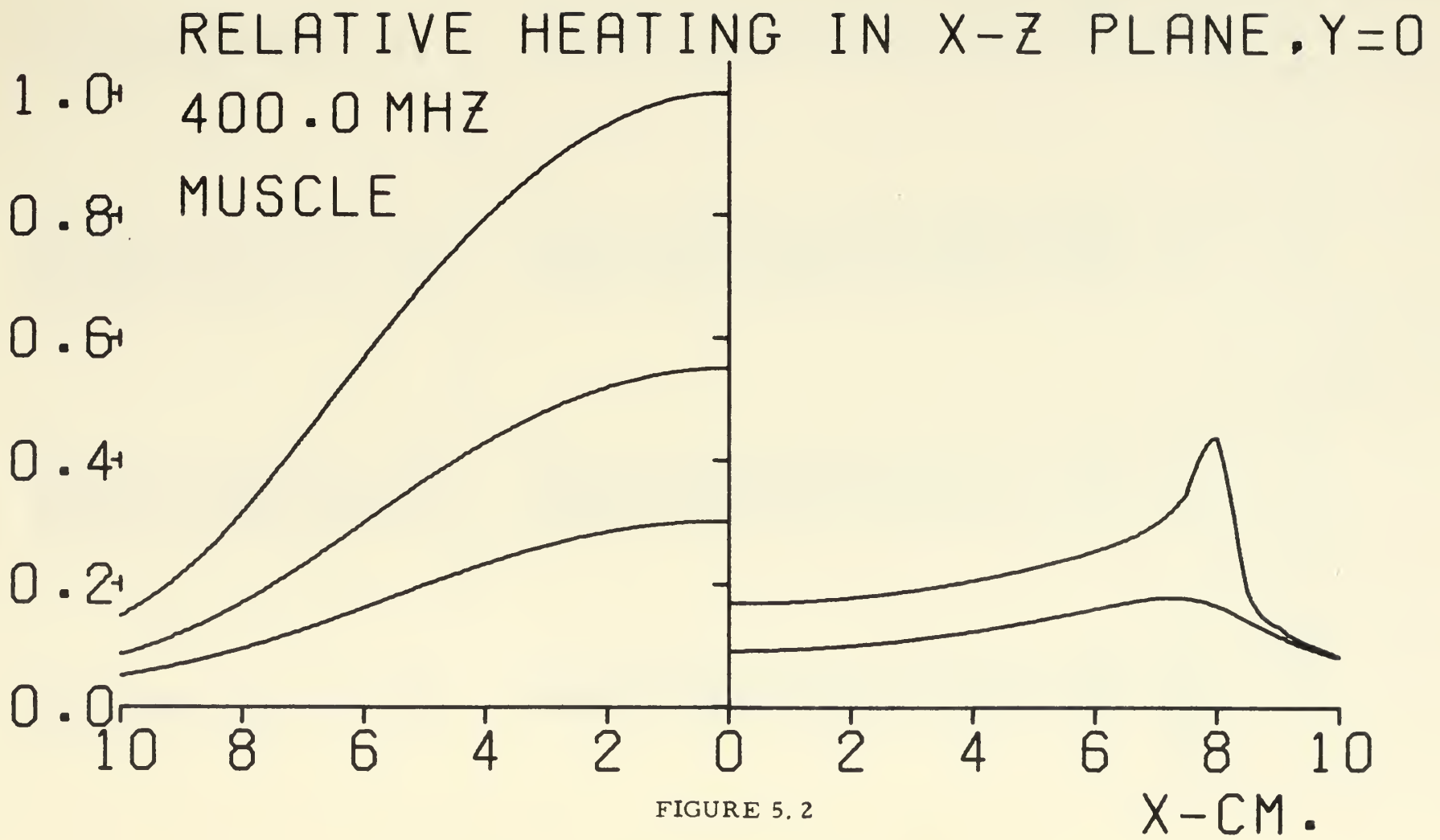

FIGURE 5.2

400 mHz GQ RHP

Table 5.3

750 MHZ

Comparison of RHPS as Computed by FFT and GQ

$Z = 0.1$ cm $Y = 0.0$ cm $Z_1 = 2.0$ cm

X	P FFT	P GAUSS	% ERROR
0.0	0.219999	0.230121	1.012
0.5	.227923	.230939	0.302
1.0	.223827	.233344	.952
1.5	.235375	.237112	.174
2.0	.233776	.241917	.814
2.5	.247462	.247393	.007
3.0	.246062	.253100	.704
3.5	.260112	.258668	.144
4.0	.256719	.263765	.705
4.5	.270403	.268169	.223
5.0	.263880	.271879	.800
5.5	.278808	.275113	.370
6.0	.269301	.278575	.927
6.5	.291805	.283724	0.808
7.0	.280616	.293975	1.336
7.5	.345529	.320156	2.537
8.0	.298479	.353216	5.474
8.5	.214655	.144184	1.047
9.0	.073904	.071551	0.235
9.5	.052573	.052983	0.041
10.0	0.037884	0.041624	0.374

$Z = 1.0$ cm $Y = 0.0$ cm $Z_1 = 2.0$ cm

0.0	0.111816	0.113543	0.173
0.5	.112691	.114293	.160
1.0	.115150	.116457	.131
1.5	.118966	.119783	.082
2.0	.213633	.123896	.026
2.5	.128689	.128342	.035
3.0	.133528	.132638	.088
3.5	.137741	.136397	.134
4.0	.140919	.139277	.164
4.5	.142974	.141132	.184
5.0	.143856	.141959	.190
5.5	.143801	.141860	.194
6.0	.142846	.140888	.196
6.5	0.140843	0.138709	.213

Table 5.3 (continued)

Z = 1.0 cm Y = 0.0 cm Z_1 = 2.0 cm

X	P FFT	P GAUSS	% ERROR
7.0	0.136485	0.133994	0.249
7.5	.216978	.123763	.321
8.0	.109112	.105312	.380
8.5	.086657	.083343	.331
9.0	.066680	.065268	.141
9.5	.050719	.051936	.122
10.0	0.037949	0.041896	0.395

Z = 2.0 cm Y = 0.0 cm Z_1 + 2.0 cm

0.0	1.000000	1.000000	0.000
0.5	0.993348	0.993783	.043
1.0	.973627	.975335	.171
1.5	.941525	.945266	.374
2.0	.898147	.904547	.640
2.5	.844959	.854473	0.951
3.0	.783711	.796589	1.288
3.5	.0716354	.732627	1.627
4.0	.644953	.664420	1.947
4.5	.571594	.593836	2.224
5.0	.498302	.522695	2.439
5.5	.426970	.452710	2.574
6.0	.359307	.385434	2.613
6.5	.296831	.322244	2.541
7.0	.240923	.264404	2.348
7.5	.192899	.213171	2.027
8.0	.153845	.169734	1.589
8.5	.124032	.134680	1.065
9.0	.102427	.107445	0.502
9.5	.087076	.086560	0.052
10.0	0.075927	0.070414	0.551

Z = 3.0 cm Y = 0.0 cm Z_1 = 2.0 cm

0.0	0.520233	0.519987	0.025
0.5	.516642	.516633	.001
1.0	.506000	.506682	.068
1.5	.488694	.490472	.178
2.0	.465339	.468543	.320
2.5	.436742	.441603	.486
3.0	.403861	.410496	.663
3.5	.367755	.376162	0.841
4.0	.329544	.339601	1.006
4.5	0.290378	0.301852	1.147

Table 5.3 (continued)

$Z = 3.0$ cm $Y = 0.0$ cm $Z_1 = 2.0$ cm

X	P FFT	P GAUSS	% ERROR
5.0	0.251410	0.263964	1.255
5.5	.213774	.226984	1.321
6.0	.178563	.191927	1.336
6.5	.146774	.159773	1.296
7.0	.119219	.131172	1.195
7.5	.096394	.106731	1.034
8.0	.078352	.086502	0.815
8.5	.064673	.070173	.550
9.0	.054853	.057157	.257
9.5	.047166	.046785	.038
10.0	0.041558	0.038461	0.310

$Z = 4.0$ cm $Y = 0.0$ cm $Z_1 = 2.0$ cm

0.0	0.270218	0.270042	0.018
0.5	.268288	.268239	.005
1.0	.262569	.262887	.032
1.5	.253261	.254162	.090
2.0	.240690	.242347	.166
2.5	.225288	.227822	.253
3.0	.207581	.211048	.347
3.5	.188166	.192560	.439
4.0	.167699	.172950	.525
4.5	.146866	.152844	.598
5.0	.126363	.132888	.652
5.5	.106861	.113707	.685
6.0	.088956	.095864	.691
6.5	.073124	.079805	.668
7.0	.059664	.065816	.615
7.5	.048675	.053989	.531
8.0	.040046	.044232	.419
8.5	.033496	.036313	.282
9.0	.028636	.029927	.129
9.5	.025039	.024768	.027
10.0	0.022295	0.020567	0.173

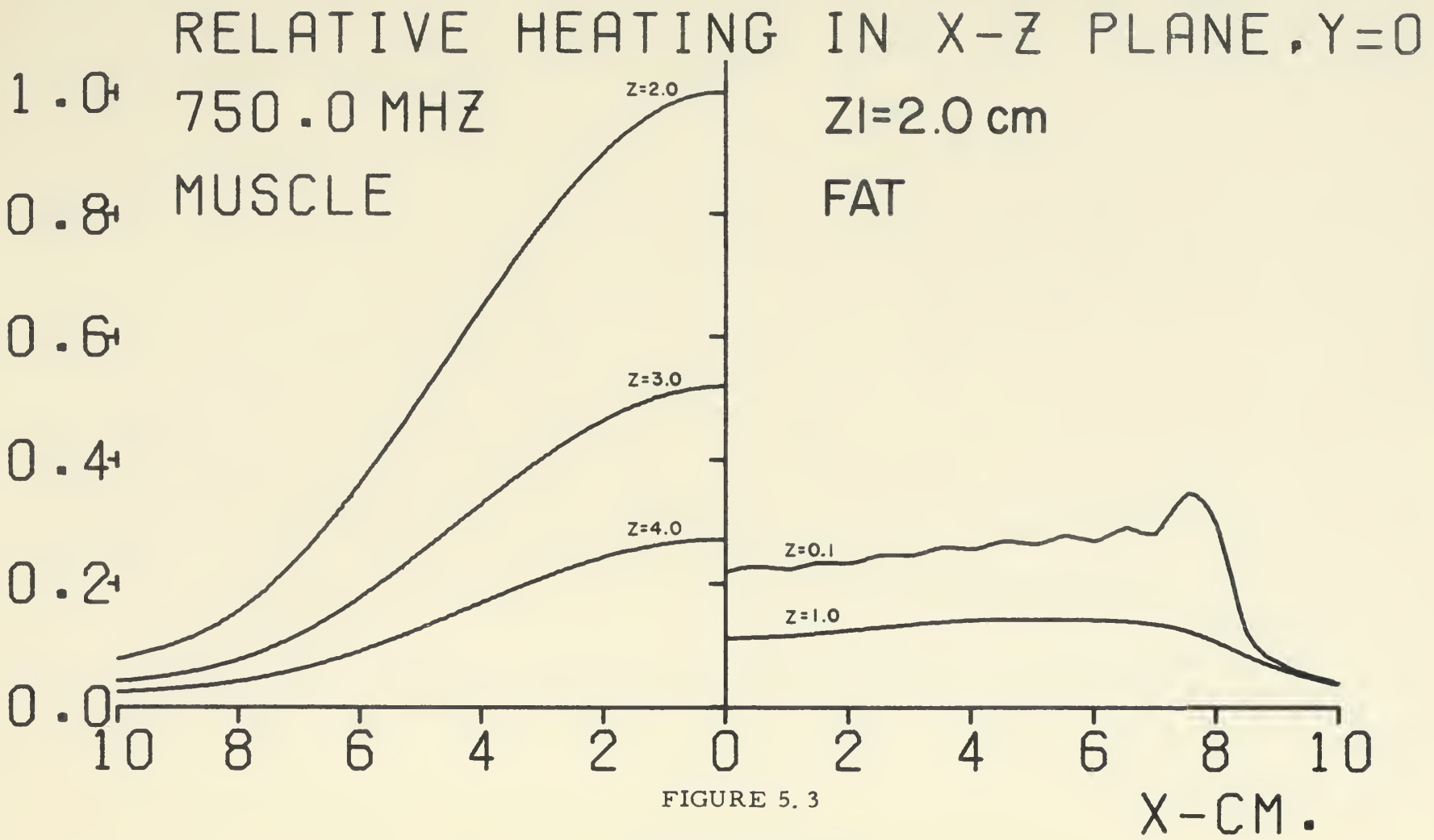

FIGURE 5.3

750 mHz FFT RHP

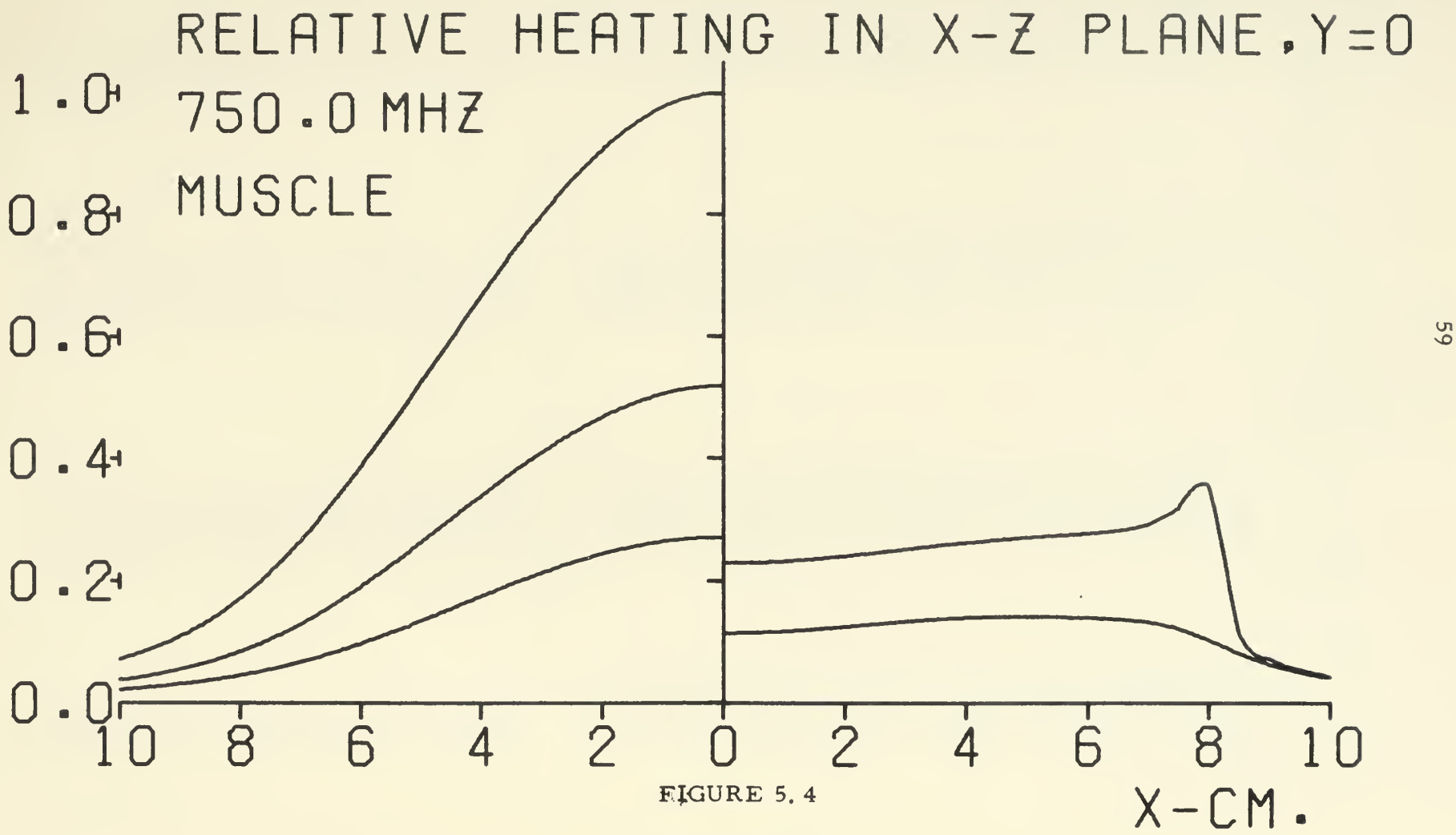

FIGURE 5.4

750 mHz GQ RHP

Table 5.4

918.8 MHZ

Comparison of RHPS as Computed by FFT and GQ

$Z = 0.1$ cm $Y = 0.0$ cm $Z_1 = 2.0$ cm

X	P FFT	P GAUSS	% ERROR
0.0	0.307665	0.319533	1.187
0.5	.318697	.320667	0.197
1.0	.312688	.323887	1.120
1.5	.328181	.328736	0.055
2.0	.324581	.334546	.997
2.5	.341489	.340525	.096
3.0	.336246	.346964	.972
3.5	.351737	.350319	0.142
4.0	.342179	.353316	1.114
4.5	.356449	.355085	0.136
5.0	.342905	.356094	1.319
5.5	.360407	.357217	0.319
6.0	.345085	.359791	1.471
6.5	.375579	.365824	0.976
7.0	.359559	.379465	1.991
7.5	.445967	.413545	3.242
8.0	.369174	.447123	7.795
8.5	.147920	.132507	1.541
9.0	.092290	.080835	1.146
9.5	.070209	.059541	1.067
10.0	0.054302	0.046853	0.745

$Z = 1.0$ cm $Y = 0.0$ cm $Z_1 = 2.0$ cm

0.0	0.144381	0.146859	0.248
0.5	.145761	.148084	.232
1.0	.149585	.151553	.197
1.5	.155298	.156693	.139
2.0	.161878	.162667	.079
2.5	.168374	.168539	.017
3.0	.173745	.173442	.030
3.5	.177413	.176752	.066
4.0	.179011	.178196	.082
4.5	.178812	.177896	.092
5.0	.177246	.176304	.094
5.5	.175111	.174003	.111
6.0	.172744	.171344	.140
6.5	.169904	.167855	.205
7.0	.164432	.161370	.306
7.5	.152263	.147447	.482
8.0	0.130205	0.122927	0.728

Table 5.4 (continued)

X	P FFT	P GAUSS	% ERROR
	Z = 1.0 cm Y = 0.0 cm Z_1 = 2.0 cm		
8.5	0.105004	0.095295	0.971
9.0	.084526	.073889	1.064
9.5	.068273	.058699	0.957
10.0	0.054134	0.047413	0.672
	Z = 2.0 cm Y = 0.0 cm Z_1 = 2.0 cm		
0.0	1.000000	1.000000	0.000
0.5	0.994130	0.994035	.010
1.0	.976754	.976381	.037
1.5	.948539	.947722	.082
2.0	.910485	.909097	.139
2.5	.863800	.861776	.202
3.0	.809766	.807131	.264
3.5	.749643	.746547	.310
4.0	.684639	.681373	.327
4.5	.615931	.612953	.298
5.0	.544743	.542659	.208
5.5	.472431	.471968	.046
6.0	.400548	.402477	.193
6.5	.330890	.335891	.500
7.0	.265553	.274031	0.848
7.5	.206994	.218845	1.185
8.0	.157785	.172206	1.442
8.5	.119638	.135132	1.549
9.0	.092391	.107008	1.462
9.5	.074256	.085977	1.172
10.0	0.062899	0.070018	0.712
	Z = 3.0 cm Y = 0.0 cm Z_1 = 2.0 cm		
0.0	0.521890	0.520860	0.103
0.5	.518547	.517491	.106
1.0	.508664	.507526	.114
1.5	.492652	.491379	.127
2.0	.471135	.469684	.145
2.5	.444872	.443222	.165
3.0	.414672	.412841	.183
3.5	.381339	.379406	.193
4.0	.345638	.343759	.188
4.5	0.308315	0.306731	0.158

Table 5.4 (continued)

$Z = 3.0$ cm $Y = 0.0$ cm $Z_1 = 2.0$ cm

X	P FFT	P GAUSS	% ERROR
5.0	0.270145	0.269174	0.097
5.5	.231993	.232008	.001
6.0	.194862	.196241	.138
6.5	.159885	.162945	.306
7.0	.128228	.133128	.490
7.5	.100900	.109544	.664
8.0	.078529	.086485	.796
8.5	.061217	.069707	.849
9.0	.048567	.056560	.799
9.5	.039859	.046257	.640
10.0	0.034219	0.038083	0.386

$Z = 4.0$ cm $Y = 0.0$ cm $Z_1 = 2.0$ cm

0.0	0.272516	0.271596	0.092
0.5	.270639	.269714	.093
1.0	.265092	.264150	.094
1.5	.256111	.255142	.097
2.0	.244061	.243057	.100
2.5	.229383	.228344	.104
3.0	.212563	.211507	.106
3.5	.194099	.193072	.103
4.0	.174496	.173578	.092
4.5	.154269	.153581	.069
5.0	.133655	.133655	.030
5.5	.114105	.114382	.028
6.0	.095295	.096325	.103
6.5	.078054	.079979	.192
7.0	.062821	.065697	.288
7.5	.049886	.053638	.375
8.0	.039362	.043751	.439
8.5	.031185	.035806	.462
9.0	.025153	.029475	.432
9.5	.020963	.024413	.345
10.0	0.018243	0.020317	0.207

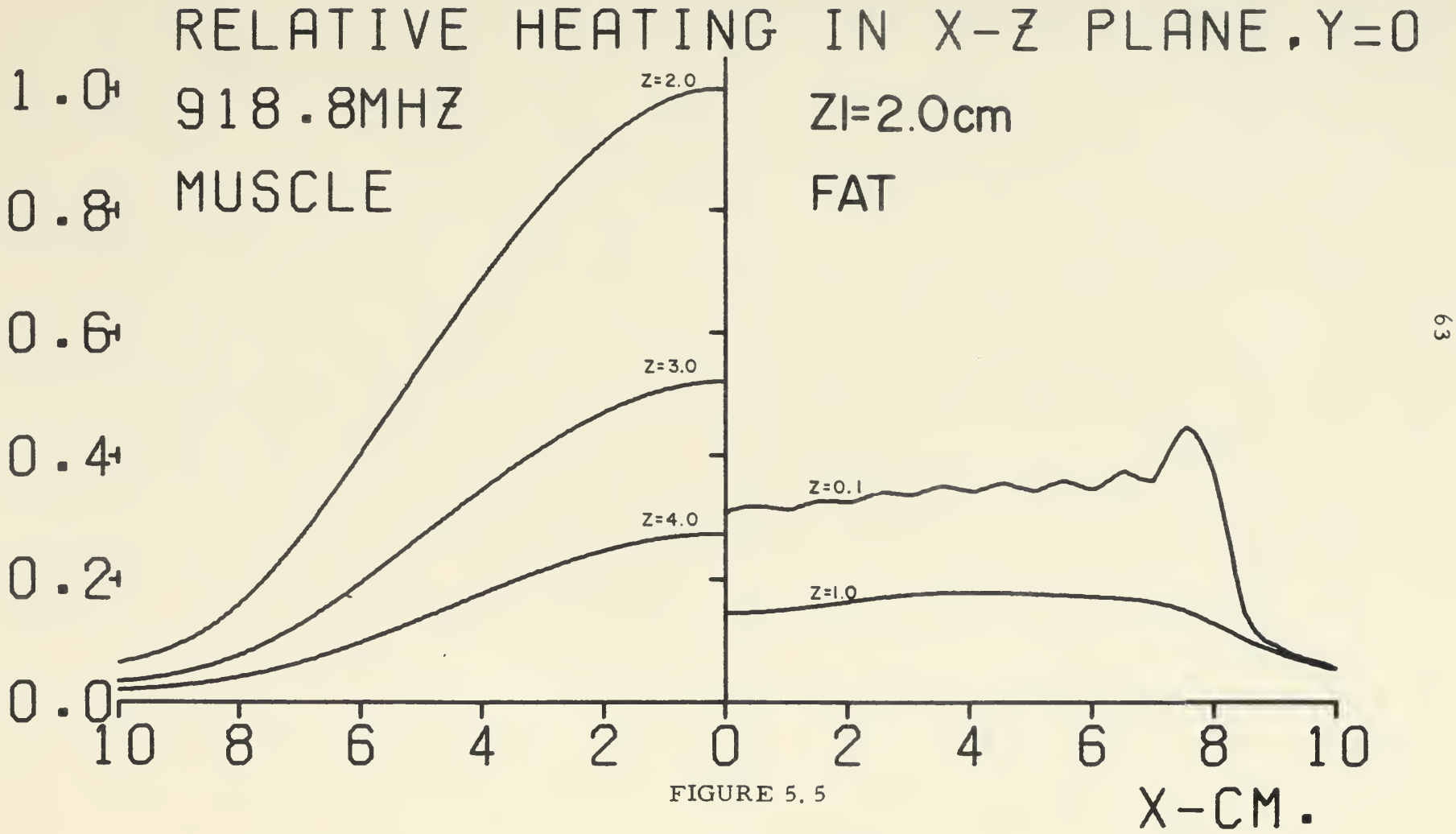

FIGURE 5.5

918.8 mHz FFT RHP

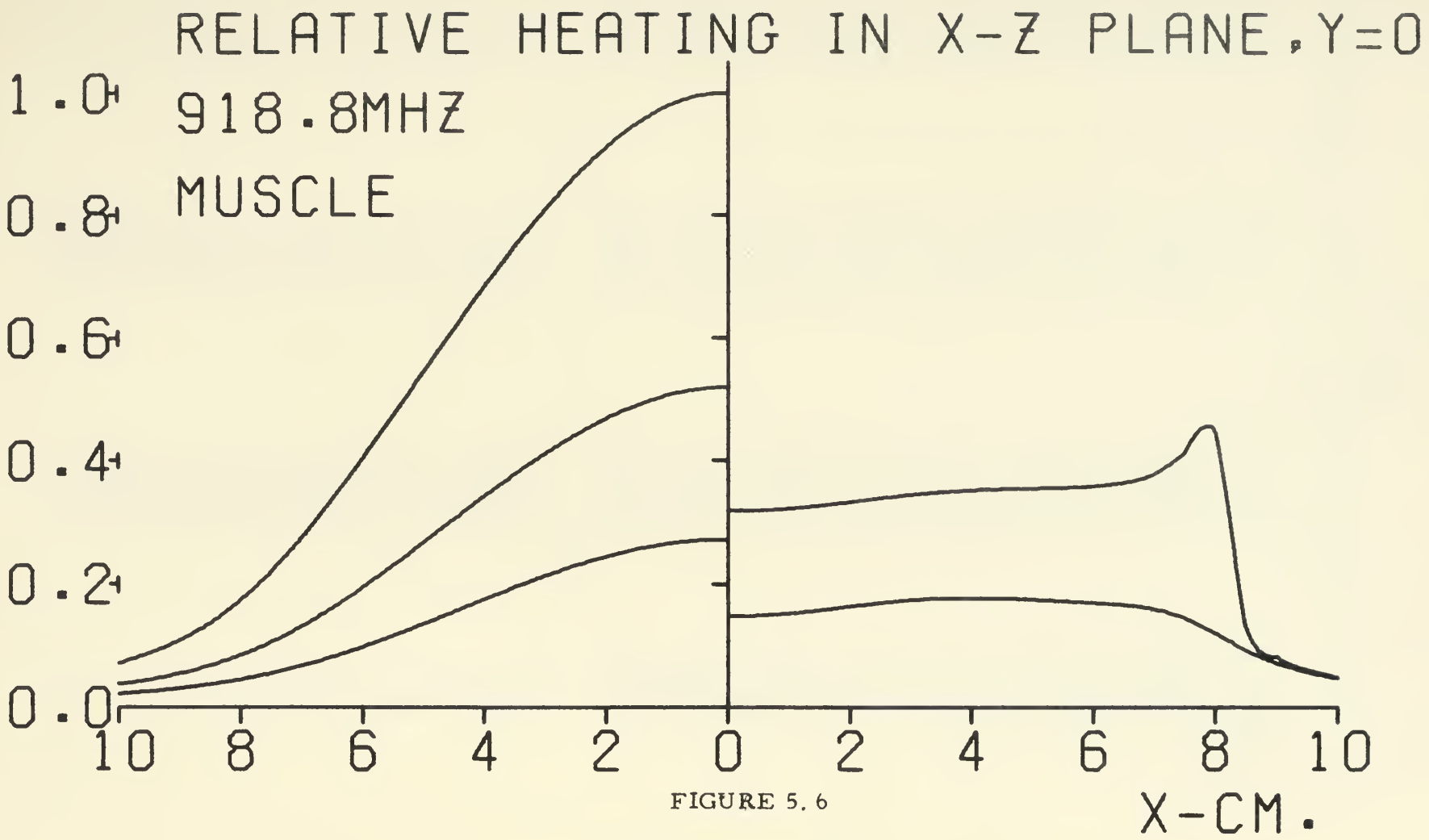

FIGURE 5.6

918.8 mHz GQ RHP

Table 5.5

1500 MHZ

Comparison of RHPS as Computed by FFT and GQ

$Z = 0.1$ cm $Y = 0.0$ cm $Z_1 = 2.0$ cm

X	P FFT	P GAUSS	% ERROR
0.0	0.769940	0.791965	2.202
0.5	.797484	.795102	0.238
1.0	.782551	.803072	2.052
1.5	.817937	.812381	0.556
2.0	.800998	.819285	1.829
2.5	.829700	.821610	0.809
3.0	.800512	.819920	1.941
3.5	.824841	.817286	0.756
4.0	.793202	.817557	2.435
4.5	.830136	.823257	0.688
5.0	.805427	.834203	2.878
5.5	.860066	.847315	1.275
6.0	.827499	.857974	3.048
6.5	.892359	.862831	2.953
7.0	.821465	.863583	4.212
7.5	.957599	.876068	8.153
8.0	.642953	.781976	13.902
8.5	.164369	.155495	0.887
9.0	.077163	.083483	0.632
9.5	.050834	.061547	1.071
10.0	0.044408	0.050588	0.618

$Z = 1.0$ cm $Y = 0.0$ cm $Z_1 = 2.0$ cm

0.0	0.371453	0.375005	0.355
0.5	.376461	.379559	.310
1.0	.389622	.391727	.210
1.5	.407001	.407720	.072
2.0	.423560	.423174	.039
2.5	.436171	.435057	.111
3.0	.443940	.442821	.112
3.5	.449051	.448231	.082
4.0	.454231	.453964	.027
4.5	.461729	.461654	.008
5.0	.470444	.470326	.012
5.5	.476507	.475855	.065
6.0	.472567	.471472	.110
6.5	.450246	.448732	.151
7.0	.400007	.398553	.145
7.5	.316297	.315145	.115
8.0	0.212149	0.212777	0.063

Table 5.5 (continued)

X	P FFT	P GAUSS	% ERROR
	Z = 1.0 cm Y = 0.0 cm Z_1 = 2.0 cm		
8.5	0.128503	0.133475	0.497
9.0	.081896	.091392	0.950
9.5	.059079	.069619	1.054
10.0	0.049324	0.056038	0.671
	Z = 2.0 cm Y = 0.0 cm Z_1 = 2.0 cm		
0.0	1.000000	1.000000	0.000
0.5	1.023147	1.022908	.024
1.0	1.090709	1.089751	.096
1.5	1.196503	1.194405	.210
2.0	1.328885	1.325446	.344
2.5	1.470068	1.465576	.449
3.0	1.597090	1.592548	.454
3.5	1.684959	1.682123	.284
4.0	1.711551	1.712660	.111
4.5	1.662959	1.670168	0.721
5.0	1.537580	1.552239	1.466
5.5	1.347428	1.369424	2.200
6.0	1.115913	1.143307	2.739
6.5	0.872545	0.901637	2.909
7.0	.646177	.672073	2.590
7.5	.458807	.476519	1.771
8.0	.321036	.327093	0.606
8.5	.230057	.224164	0.589
9.0	.172774	.158535	1.424
9.5	.133854	.117790	1.606
10.0	0.102661	0.091728	1.093
	Z = 3.0 cm Y = 0.0 cm Z_1 = 2.0 cm		
0.0	0.445169	0.443357	0.181
0.5	.454701	.452869	.183
1.0	.482492	.480589	.190
1.5	.525897	.523858	.204
2.0	.579906	.577710	.220
2.5	.636850	.634624	.223
3.0	.686838	.684962	.188
3.5	.719186	.718322	.086
4.0	.724650	.725647	.100
4.5	0.697849	0.701516	0.367

Table 5.5 (continued)

Z = 3.0 cm Y = 0.0 cm Z_1 = 2.0 cm

X	P FFT	P GAUSS	% ERROR
5.0	0.639040	0.645835	0.679
5.5	.554515	.564262	0.975
6.0	.455316	.467056	1.174
6.5	.354539	.366590	1.205
7.0	.263993	.274248	1.025
7.5	.191319	.197768	0.645
8.0	.138623	.139991	.137
8.5	.103130	.099480	.365
9.0	.079439	.072423	.702
9.5	.062145	.054623	.752
10.0	0.047676	0.042668	0.501

Z = 4.0 cm Y = 0.0 cm Z_1 = 2.0 cm

0.0	0.198890	0.197535	0.135
0.5	.202728	.201401	.133
1.0	.213910	.212657	.125
1.5	.231335	.230181	.115
2.0	.252897	.251864	.103
2.5	.275344	.274490	.085
3.0	2.94464	.293935	.053
3.5	.305738	.305781	.004
4.0	.305365	.306291	.093
4.5	.291365	.293457	.209
5.0	.264338	.267719	.338
5.5	.227505	.232026	.452
6.0	.185905	.191090	.518
6.5	.144990	.150078	.509
7.0	.109152	.113250	.410
7.5	.080784	.083091	.231
8.0	.060134	.060205	.007
8.5	.045859	.043822	.204
9.0	.035893	.032519	.337
9.5	.028277	.024815	.346
10.0	0.021741	0.019488	0.225

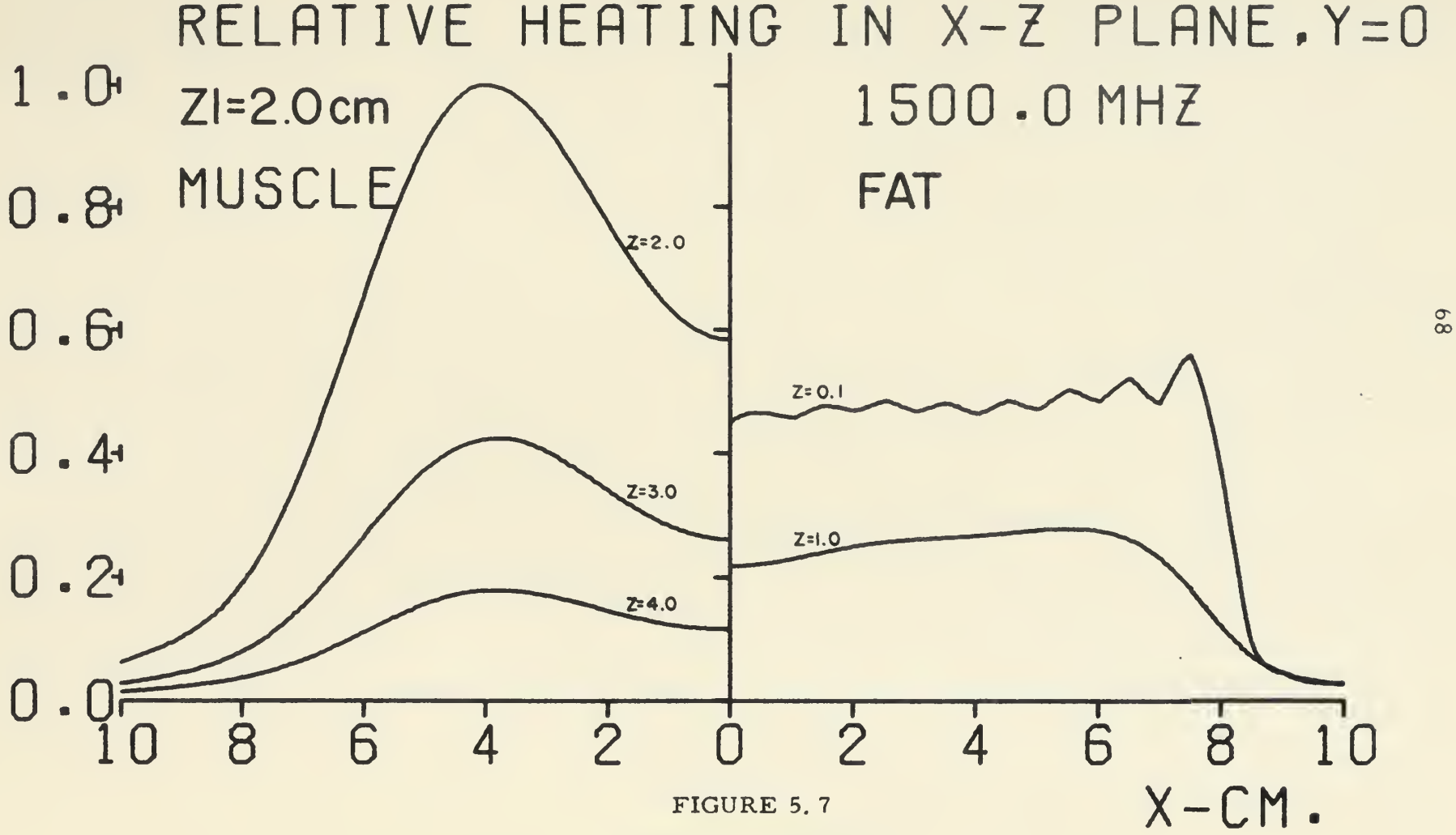

FIGURE 5.7

1500 mHz FFT RHP

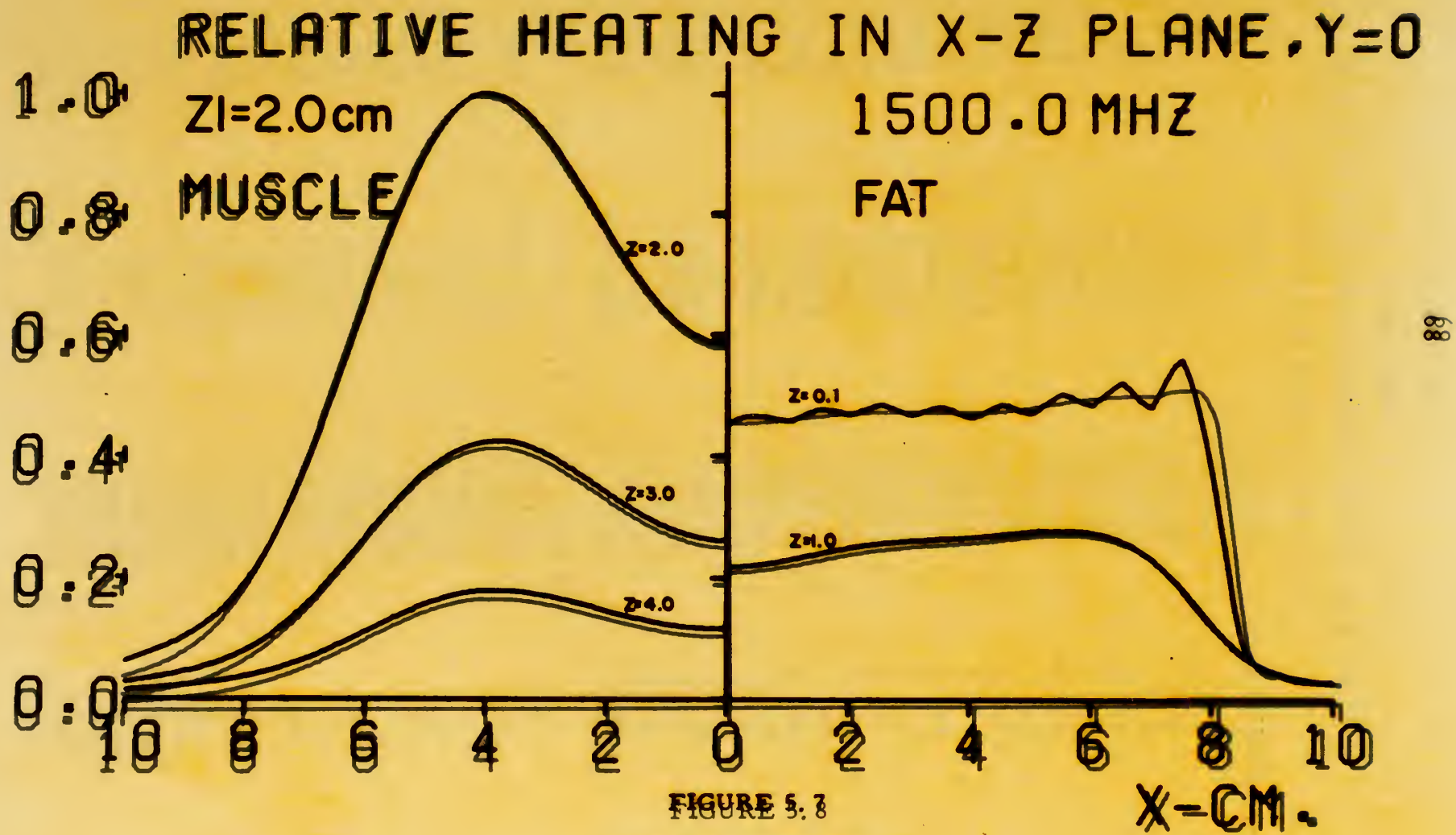

FIGURE 5.7

FIGURE 5.8

1500 mHz FFT RHP

1500 mHz GE RHP

Table 5.6

2450 MHZ

Comparison of RHPS as Computed by FFT and GQ

$Z = 0.1$ cm $Y = 0.0$ cm $Z_1 = 2.0$ cm

X	P FFT	P GAUSS	% ERROR
0.0	0.366811	0.377543	1.073
0.5	.378686	.378658	0.002
1.0	.370445	.380583	1.014
1.5	.381763	.380782	0.098
2.0	.368881	.378765	0.988
2.5	.378281	.376830	0.145
3.0	.366957	.377359	1.040
3.5	.382005	.380061	0.194
4.0	.370698	.382443	1.174
4.5	.384621	.382672	0.195
5.0	.367049	.381338	1.429
5.5	.383721	.380048	0.367
6.0	.363116	.378770	1.565
6.5	.386408	.375910	1.050
7.0	.351085	.372131	2.105
7.5	.407494	.376310	3.118
8.0	.270671	.335005	6.433
8.5	.056666	.052222	0.444
9.0	.015730	.015568	0.016
9.5	.004814	.006221	0.141
10.0	0.004538	0.004280	0.026
	$Z = 1.0$ cm $Y = 0.0$ cm $Z_1 = 2.0$ cm		
0.0	0.468521	0.471441	0.292
0.5	.468444	4.71251	.281
1.0	.466835	.469570	.273
1.5	.461953	.464718	.276
2.0	.454289	.457362	.307
2.5	.447671	.450967	.330
3.0	.445632	.449004	.337
3.5	.448780	.451928	.315
4.0	.454143	.457113	.297
4.5	.458535	.461291	.276
5.0	.459520	.462096	.258
5.5	.454628	.456684	.206
6.0	.437820	.439293	.147
6.5	.400307	.401186	.088
7.0	.333693	.334352	.066
7.5	.238406	.238807	.040
8.0	0.135304	0.135515	0.021

Table 5.6 (continued)

Z = 1.0 cm Y = 0.0 cm Z_1 = 2.0 cm

X	P FFT	P GAUSS	% ERROR
8.5	0.061793	0.062571	0.078
9.0	.026235	.027940	.170
9.5	.012791	.014218	.143
10.0	0.009203	0.008925	0.028
	Z = 2.0 cm Y = 0.0 cm Z_1 = 2.0 cm		
0.0	1.000000	1.000000	0.000
0.5	0.974299	0.975367	.107
1.0	.907962	.911726	.376
1.5	.827885	.834780	.689
2.0	.764870	.774094	.922
2.5	.742358	.752317	.996
3.0	.770501	.779319	.882
3.5	.844159	.850125	.597
4.0	0.942362	0.944446	2.08
4.5	1.030636	1.029071	.156
5.0	1.069843	1.066413	.343
5.5	1.031177	1.028739	.244
6.0	0.910033	0.911293	.126
6.5	.729405	.735520	.611
7.0	.529529	.539328	0.980
7.5	3.49858	.360162	1.030
8.0	2.14015	.221086	0.707
8.5	.125118	.126845	.173
9.0	.072054	.069551	.250
9.5	.040644	.037550	.309
10.0	0.021492	0.020903	0.059
	Z = 3.0 cm Y = 0.0 cm Z_1 = 2.0 cm		
0.0	0.336450	0.336431	0.002
0.5	.328117	.328459	.034
1.0	.306858	.308100	.124
1.5	.281932	.284187	.225
2.0	.263677	.266633	.296
2.5	.259506	.262592	.309
3.0	.271936	.274521	.258
3.5	.298187	.299738	.155
4.0	.330361	.330614	.025
4.5	0.356574	0.355712	0.086

Table 5.6 (continued)

Z = 3.0 cm Y = 0.0 cm Z_1 = 2.0 cm

X	P FFT	P GAUSS	% ERROR
5.0	0.364210	0.362930	0.128
5.5	.345055	.344363	.069
6.0	.299617	.300374	.076
6.5	.237352	.239797	.245
7.0	.172072	.175620	.355
7.5	.115545	.118996	.345
8.0	.073442	.075554	.211
8.5	.045381	.045594	.021
9.0	.027663	.026528	.114
9.5	.016311	.015152	.116
10.0	0.008900	0.008750	0.015

Z = 4.0 cm Y = 0.0 cm Z_1 = 2.0 cm

0.0	0.112552	0.112567	0.002
0.5	.109977	.110109	.013
1.0	.103513	.103932	.042
1.5	.096233	.096963	.073
2.0	.091462	.092384	.092
2.5	.091393	.092313	.092
3.0	.096492	.097207	.071
3.5	.105481	.105839	.036
4.0	.115526	.115471	.006
4.5	.122703	.122331	.037
5.0	.123146	.122714	.043
5.5	.114733	.114582	.015
6.0	.098312	.098701	.039
6.5	.077386	.078339	.095
7.0	.056350	.057606	.126
7.5	.038536	.039656	.112
8.0	.025298	.025886	.059
8.5	.016291	.016220	.007
9.0	.010346	.009866	.048
9.5	.006315	.005900	.042
10.0	0.003554	01003536	0.002

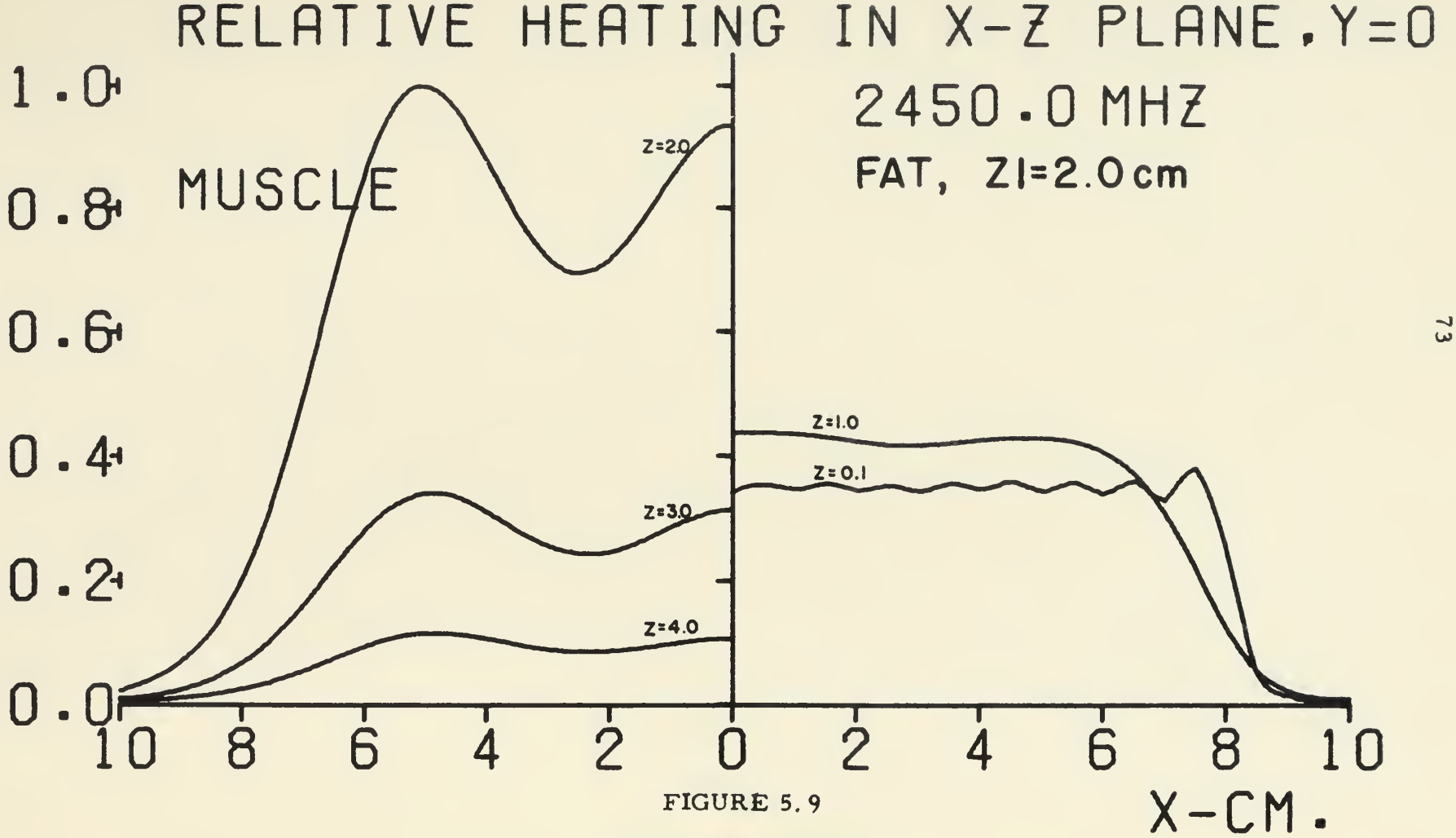

FIGURE 5.9

2450 mHz FFT RHP

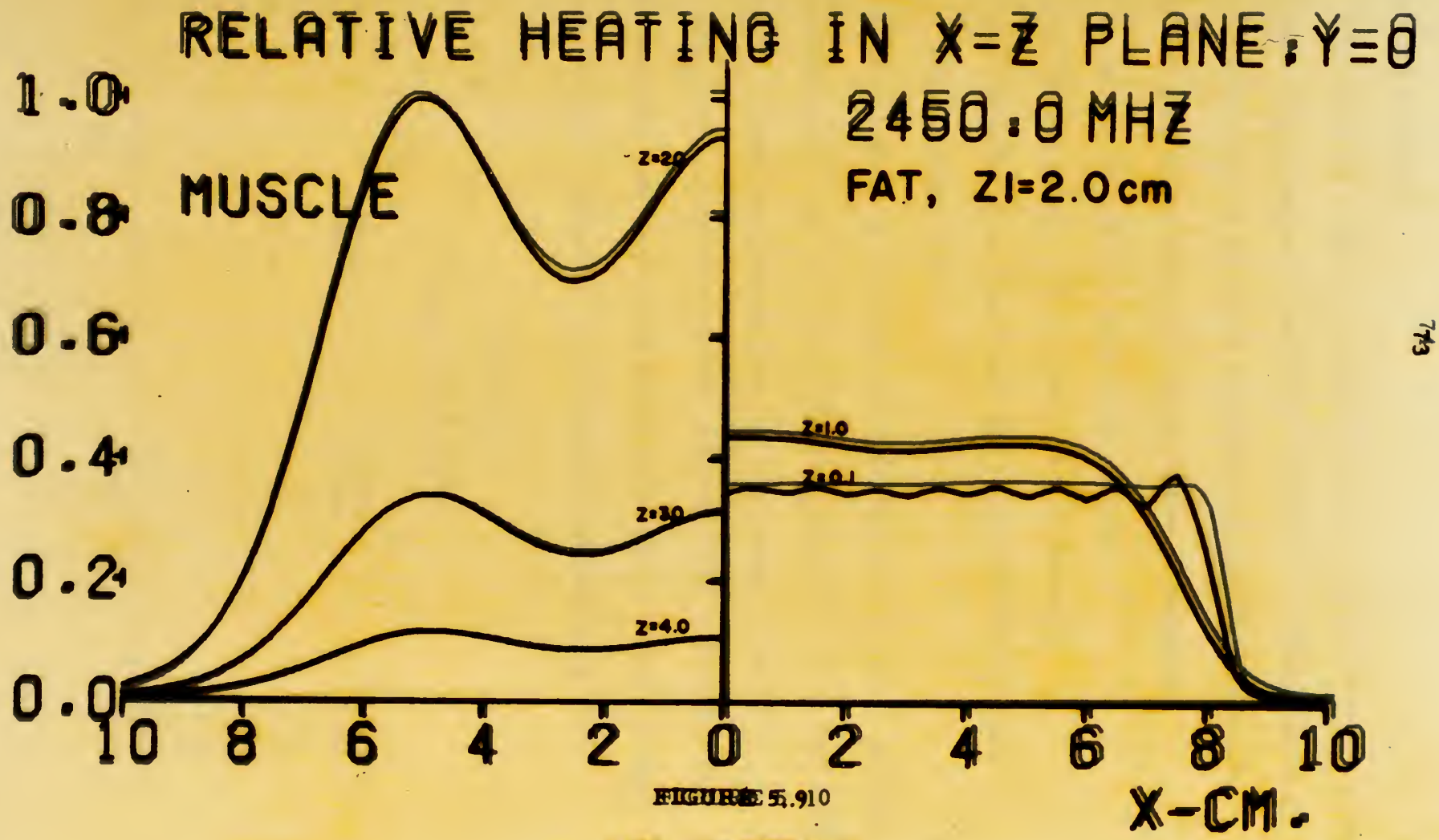

FIGURE 5.910

2450 mHz FAT RHP

5.4 Analysis of Results

The different ranges of % ERROR and the number of points lying within the various ranges are tabulated in Table 5.7. Examination of the six compared points which lie outside the range of acceptability reveals that each of the points has three factors in common

a. all occur near the edge of the aperture,

b. all occur when Z = 0.1 cm, i.e., Z is small,

c. all occur in an area where the relative heating pattern has a steep slope.

It was mentioned in section 2.6 that points in the area defined by (a) and (b) above may need corrections to account for less than infinite integration. These corrections have not been made in the FFT.

Since only 1.14% of the points compared fail to meet the 5% ERROR criterion and since all of these points are in an area of steep slope, the FFT is, therefore, an acceptable computational tool.

TABLE 5.7

Ranges of % ERROR

% ERROR			
Greater Than	But Less Than	Number of Points	Percentage in Range
10%	--	2	0.38
5	10%	4	0.76
4	5	8	1.52
3	4	17	3.24
2	3	34	6.48
1	2	71	15.05
0	1	381	72.57
Total		525	100.00%

5.5 Cost Analysis

In Chapter 3 it was stated that the fast Fourier transform is an extremely efficient method of performing discrete Fourier transforms. In this light, two further points are noteworthy in a comparison of the FFT and the Guassian guadrature.

First, all of the computed results in this chapter were performed on the CDC 6400 using the RUN (S) compiler. On the basis of central processor time only, an average time was taken, over several thousand points, for the compution of one point with the following results for the two methods,

Gaussian guadrature = 1.9306 sec./point 5.5.1

Fast Fourier transform = 0.01499 sec./point. 5.5.2

This yields a time savings factor (TSF) of

$$TSF = \frac{0.01499}{1.93062} = \frac{1}{128.8}$$

which is 76% of the theoretical TSF derived in Chapter 3.

The second point which makes the FFT not only acceptable but also desirable is that the FFT computes 4096 points for each x-y plane investigated. These points are, for a given Z, in the range

$$-16\text{cm} \leq x \leq 16\text{cm} \qquad -16\text{cm} \leq y \leq 16\text{cm}.$$

By contrast, the Gaussian guadrature computes only 21 points, for a given Z, in the range

$$y = 0 \qquad 0 \leq x \leq 10\text{cm}$$

The advantages of the FFT are, therefore:

a.) reasonably comparable accuracy,

b.) greater time savings,

c.) more complete data,

d.) no restrictions on aperture distributions.

CHAPTER 6

CONCLUSION

6.1 The FFT in Current Applications

Current development of a safe, efficient, direct contact diathermy applicator for use in treatment of musculoskeletal disorders assumes, for analysis of the electromagnetic fields, a linear superposition of an infinite set of plane wave solutions. The general solutions of the scalar wave equation thus obtained develop a complete set of Fourier transform pairs which completely specify the electromagnetic field components throughout the volume of the human tissue model.

In the past, the Fourier transforms have been computed by the Gaussian quadrature method. Economical use of the Gaussian quadrature imposed definite restrictions on the solutions thus obtained:

a.) All theoretical and empirical solutions were forced to have complete symmetry about the x and y axes thus enabling integration in only one quadrant of the u - v plane.

b.) The economics of computer time dictated that the relative heating be computed only along the positive y-axis in any desired z-plane.

c.) Extensive corrections were required near the edges of the aperture.

These restrictions obviously limited the generality and completeness of any relative heating patterns thus obtained.

The fast Fourier transform package developed in this research completely circumvents these severe restrictions. Integration is performed over all four quadrants of the u - v plane, thus eliminating the need for symmetry. In addition, the efficiency of the fast Fourier transform allows the computation of 4096 points in each z-plane rather than just a few points along an axis of symmetry. Further, even though no corrections are included in the fast Fourier transform package, nearly ninety-nine percent of all points calculated agree, to a reasonable degree, with answers from the Gaussian quadrature method. The FFT, on a point for point basis, accomplishes all of this in two orders of magnitude less time. Two minor disadvantages are encountered in the use of the fast Fourier transform. Some aliasing is encountered in z-planes near the aperture and somewhat more actual computer time is required for the computation of each z-plane. Nevertheless, these disadvantages are overwhelmingly outweighed by the completeness of the relative heating patterns obtained by the FFT.

6.2 Future Application of the FFT

Although the FFT has at this point only been adapted to the analysis of relative heating in planar models of human tissue, the package developed in this research should be extremely useful to Ho[23] in analyzing relative heating in cylindrical models.

Quantitative studies in the adverse effects of electromagnetic radiation will result in the establishment of radiation safety standards.

These quantitative studies will require an analysis of the electromagnetic fields in both planar and cylindrical models of human tissue. The fast Fourier transform package developed in this research can be easily adapted to this problem since no symmetry is required in the arrays to be transformed.

These and other problems requiring Fourier analysis in two dimensions can be implemented by replacing the SCRPEX and JAMXX subroutines by appropriate subroutines which build the two-dimensional arrays to be transformed.

APPENDIX A

SUBROUTINE NUMGEN

This subroutine utilizes that portion of Eguchi's[21] program which generates the weighing factors, W^{nk}, for each node in the transform and calculates the size and beginning and ending values for the DO loops used to transform each array. The arrays built by NUMGEN are called by FAST in Appendix B.

If the number of data points is consistent for all uses of this package, NUMGEN need only be used the first time the package is used. In the first run, the arrays built by NUMGEN can be punched out and read in as data in subsequent runs. This will result in slightly less central processor time and somewhat more peripheral processor time which is desirable on the CDC 6400. Data transmission is via labeled common.

```
      SUBROUTINE NUMGEN
      DIMENSION NUM(64,6),NNP(6),NRANG1(32,6),NRANG2(32,6),NLOOPS(6)
      DIMENSION NUNSC(64),NN(12),NM(12),NNX(64)
      COMPLEX W(32)
      COMPLEX WEXP,WW
      INTEGER GAMMA,GAM2,A,AN
      COMMON /BLOCK1/ NUM,NNP,NRANG1,NRANG2,NLOOPS,NUNSC,NN,NM,NNX,W
      COMMON /BLOCK2/ GAMMA,GAM2,NDATA,NDAT
      COMMON/FICKON/C,PI,PI2,PI22,AJ,E1,E2,AK,AKSQ,AKSQE1,AKSQE2,AKRTEF
     1AKRTEM,AKSQEF,ZI,Z,V,U,EX,INDEX,OUTPUT,AED,BED
      NDATA=2**GAMMA
      NDAT=NDATA/2
      GAM2=2*GAMMA
C     FIND THE EXPONENTS THAT W MUST BE RAISED TO FOR EACH NODE
      WEXP=CMPLX(0.0,-2.0*PI/FLOAT(NDATA))
      WW=CEXP(WEXP)
      W(1)=CMPLX(1.0,0.0)
      DO9N=2,NDAT
9     W(N)=WW**(N-1)
C     CONVERT K TO BINARY
      DO80L=1,GAMMA
      DO79K=1,NDATA
      I=0
      A=K-1
10    I=I+1
      IF(I.GT.GAMMA)GOTO39
      IF(A.EQ.0)GOTO27
      N=A/2
      AN=N*2
      IF(A.EQ.AN)NN(I)=0
      IF(A.NE.AN)NN(I)=1
      A=N
      GOTO10
C     SHIFT K IN BINARY GAMMA-NARRAY PLACES TO THE RIGHT
27    DO28KK=I,GAMMA
28    NN(KK)=0
39    CONTINUE
      LL1=GAMMA+1
      LL2=2*GAMMA
```

```
      DO35J=LL1,LL2
35    NN(J)=0
      NSHIFT=GAMMA-L
      DO36J=1,GAMMA
      NSJ=NSHIFT+J
36    NN(J)=NN(NSJ)
C     REVERSE BIT POSITIONS
      DO49J=1,GAMMA
49    NM(J)=NN(J)
      DO 450 J=1,GAMMA
      NG1J=GAMMA-J+1
450   NN(J)=NM(NG1J)
C     CONVERT BINARY BACK TO DECIMAL
      NUM(K,L)=NN(1)+1
      DO 460 J=2,GAMMA
460   NUM(K,L)=NN(J)*(2**(J-1))+NUM(K,L)
79    CONTINUE
80    CONTINUE
C     CALCULATE THE SIZE AND STARTING AND ENDING VALUES FOR THE LOOPS
C     USED TO CALCULATE THE NEW X ARRAY FOR EACH ARRAY
      DO 401 L=1,GAMMA
      IF(L.EQ.GAMMA)NNP(L)=1
      IF(L.NE.GAMMA)NNP(L)=2**(GAMMA-L)
      IF(L.EQ.1)NLOOPS(L)=1
      IF(L.NE.1)NLOOPS(L)=2**(L-1)
      LOOPS=NLOOPS(L)
      DO 400 LOOPN=1,LOOPS
      NRANG1(LOOPN,L)=(2*LOOPN-2)*NNP(L)+1
400   NRANG2(LOOPN,L)=(2*LOOPN-1)*NNP(L)
401   CONTINUE
```

```
C       CONVERT DECIMAL TO BINARY, REVERSE BIT POSITIONS AND CONVERT
C       BACK TO DECIMAL
        DO200JJ=1,NDATA
        I=0
        A=JJ-1
411     I=I+1
        IF(I.GT.GAMMA)GOTO130
        IF(A.EQ.0)GOTO127
        N=A/2
        AN=N*2
        IF(A.EQ.AN)NN(I)=0
        IF(A.NE.AN)NN(I)=1
        A=N
        GOTO411
127     DO128KK=I,GAMMA
128     NN(KK)=0
130     CONTINUE
        DO440J=1,GAMMA
440     NM(J)=NN(J)
        DO150J=1,GAMMA
        JG=GAMMA+1-J
150     NN(J)=NM(JG)
        NUNSC(JJ)=NN(1)+1
        DO160J=2,GAMMA
160     NUNSC(JJ)=NN(J)*(2**(J-1))+NUNSC(JJ)
200     CONTINUE
        RETURN
        END
```

APPENDIX B

SUBROUTINE FAST

Subroutine FAST utilizes that portion of Eguchi's[21] program which calls the subroutine FFT from the bit reversed address arrangement. FFT is the actual workhorse that performs the Fourier transformation. Data transmission is via labeled common.

```
      SUBROUTINE FAST
      COMPLEX XT(64,64)
      DIMENSION NUNSC(64),NN(12),NM(12),NNX(64)
      DIMENSION NUM(64,6),NNP(6),NRANG1(32,6),NRANG2(32,6),NLOOPS(6)
      COMPLEX X(64),XP(64),W(32),XN1,XN2
      INTEGER GAMMA,GAM2,A,AN
      COMMON /BLOCK1/ NUM,NNP,NRANG1,NRANG2,NLOOPS,NUNSC,NN,NM,NNX,W
      COMMON /BLOCK2/ GAMMA,GAM2,NDATA,NDAT
      COMMON /BLOCK3/ XT,X,XP
C     TRANSFORMTHE XT ARRAY BY ROWS
      DO211M=1,NDATA
      DO210N=1,NDATA
210   X(N)=XT(M,N)
      CALL FFT
      DO205N=1,NDATA
205   XT(M,N)=X(N)
211   CONTINUE
C     TRANSFORM THE XT ARRAY BY COLUMNS
      DO220N=1,NDATA
      DO213M=1,NDATA
213   X(M)=XT(M,N)
      CALL FFT
      DO216M=1,NDATA
216   XT(M,N)=X(M)/CMPLX(FLOAT(NDATA),0.0)
220   CONTINUE
C     REARRANGE THE XT ARRAY INTO STANDARD FORM FROM THE BIT
C     REVERSED ADDRESS FORM
      DO90M=1,NDAT
      DO87N=1,NDAT
      XN1=XT(M,N)
      XT(M,N)=XT(M+32,N+32)
      XT(M+32,N+32)=XN1
      XN2=XT(M,N+32)
      XT(M,N+32)=XT(M+32,N)
87    XT(M+32,N)=XN2
90    CONTINUE
      RETURN
      END
```

```
      SUBROUTINE FFT
      DIMENSION NUNSC(64),NN(12),NM(12),NNX(64)
      DIMENSION NUM(64,6),NNP(6),NRANG1(32,6),NRANG2(32,6),NLOOPS(6)
      COMPLEX XT(64,64)
      COMPLEX X(64),XP(64),W(32),XN1,XN2
      COMPLEX XHOLD,WNX
      INTEGER GAMMA,GAM2,A,AN
      COMMON /BLOCK1/ NUM,NNP,NRANG1,NRANG2,NLOOPS,NUNSC,NN,NM,NNX,W
      COMMON /BLOCK2/ GAMMA,GAM2,NDATA,NDAT
      COMMON /BLOCK3/ XT,X,XP
C     ACTUAL TRANSFORMATION TAKES PLACE IN THIS SUBROUTINE
      DO5K=1,NDATA
5     XP(K)=X(K)
      DO10NARRAY=1,GAMMA
      LOOPS=NLOOPS(NARRAY)
      DO9NLOOP=1,LOOPS
      MRANG1=NRANG1(NLOOP,NARRAY)
      MRANG2=NRANG2(NLOOP,NARRAY)
      DO8NODE1=MRANG1,MRANG2
      NPWR=NUM(NODE1,NARRAY)
      NODE2=NODE1+NNP(NARRAY)
      WNX=W(NPWR)*XP(NODE2)
      XHOLD=XP(NODE1)
      XP(NODE1)=XHOLD+WNX
8     XP(NODE2)=XHOLD-WNX
9     CONTINUE
10    CONTINUE
      DO20NODE=1,NDATA
      NNZ=NUNSC(NODE)
20    X(NNZ)=XP(NODE)
      RETURN
      END
```

APPENDIX C

SUBROUTINE SCRPEX

Subroutine SCRPEX calculates the Fourier transform of a theoretical aperture distribution for a given u and v. In Chapter 2, the final set of equations for the relative heating problem contained a ξ which was the Fourier transform of the aperture distribution at $z = 0^-$. This subroutine is entered into the package as a separate entity to enable a potential user to change aperture distributions without rewriting the JAMXX subroutine. Data transmission is via labeled common.

```
      SUBROUTINE SCRPEX
      COMPLEX AJ,E1,E2,AKSQE1,AKSQE2,EX,OUTPUT
      COMMON/PICKON/C,PI,PI2,PI22,AJ,E1,E2,AK,AKSQ,AKSQE1,AKSQE2,AKRTEM
     1,AKRTEM,AKSQEF,Z1,Z,V,U,EX,INDEX,OUTPUT,AED,BED
      AV=AED*V
      BU=BED*U
      AVS=AV**2
C     CHECK FOR DISCONTINUITIES IN THE FUNCTION
      IF(PI22.EQ.AVS.AND.U.EQ.0.)GOTO30
      IF(U.EQ.0.)GOTO10
      IF(PI22.EQ.AVS)GOTO20
C     IF EVERYTHING IS OK, EX IS GIVEN BY
      EX=SIN(BU)*COS(AV)/(BU*(AVS-PI22))
      RETURN
C     IF U=0, EX IS GIVEN BY
10    EX=COS(AV)/(AVS-PI22)
      RETURN
C     IF(PI/2=AV/2),THEN EX IS GIVEN BY
20    EX=SIN(BU)/(PI*BU)
      RETURN
C     IF BOTH DISCONTINUITIES APPEAR SIMULTANEOUSLY, EX IS GIVEN BY
30    EX=1./PI
      RETURN
      END
```

APPENDIX D

SUBROUTINE JAMXX

JAMXX computes the appropriate value in the u - v plane for the array which is to be transformed. JAMXX requires an input from SCRPEX which, for a given u and v, corresponds to the Fourier transform of the aperture distribution. This subroutine by McDougall[11] incorporates all the theory of Chapter 2 except the corrections and ξ, the aperture distribution transform. Data transmission is accomplished via labeled common.

```
      SUBROUTINE JAMXX
      COMPLEX AJ,E1,E2,AKSQE1,AKSQE2,W2,W1,W1SQ,W2SQ,EWIZ1,EWIZ12,EW2Z1
     1APM1,APM2,BPM1,BPM2,CPM1,CPM2,EWIZ,EX,AP,AM,BP,BM,CP,CM,FMZ0,EW2Z
     2FMZ1,GPZ1,FPM1,FPM2,FP,FM,GPM1,GPM2,GP,GM,OUTPUT,TWIZ1
      COMMON/PICKON/C,PI,PI2,PI22,AJ,E1,E2,AK,AKSQ,AKSQE1,AKSQE2,AKRTEF
     1AKRTEM,AKSQEF,Z1,Z,V,U,EX,INDEX,OUTPUT,AED,BED
C     THIS SUBROUTINE IS EASILY TRANSLATED IF THE EQUATIONS ARE
C     RELATED TO THOSE DISCUSSED IN CHAPTER TWO.  MOST OF THE
C     VARIABLES HAVE THE IDENTICAL NAMES GIVEN THEM IN CHAPTER 2.
      VSQ=V*V
      USQ=U*U
      UVSQ=USQ*VSQ
      XI2=USQ+VSQ
      XI=SQRT(XI2)
      IF(XI.LE.AKRTEF)GOTO26
      IF(XI.LE.AKRTEM)GOTO24
      W2=AJ*CSQRT(XI2-AKSQE2)
      GOTO25
24    CONTINUE
      W2=-CSQRT(AKSQE2-XI2)
25    CONTINUE
      W1=AJ*CSQRT(XI2-AKSQE1)
      GOTO27
26    CONTINUE
      W1=-CSQRT(AKSQE1-XI2)
      W2=-CSQRT(AKSQE2-XI2)
27    CONTINUE
      W1SQ=W1*W1
      W2SQ=W2*W2
      EWIZ1=AJ*W1*Z1
      EWIZ1=CEXP(EWIZ1)
      EWIZ12=EWIZ1**2
      TWIZ1=-AJ*((EWIZ1-1.0)/(EWIZ1+1.0-(2.0*EWIZ1/(EWIZ1+1.0))))
      EW2Z1=AJ*W2*Z1
      EW2Z1=CEXP(EW2Z1)
      APM1=W1*W2*AKSQE2
      APM2=-UVSQ+(W1SQ+USQ)*(W2SQ+VSQ)
      AP=APM1+APM2
      AM=APM1-APM2
```

APPENDIX E

SAMPLE PROGRAM

The sample program was used to calculate the relative heating patterns in Figure E.1. It utilizes all of the subroutines in the previous appendices in the manner outlined in Figure 4.1. Figure E.1 is a CALCOMP plot of some of the wealth of information in each transformed array. This figure shows the relative heating pattern for various y's at the fat-muscle interface for 2450 mHz. It should be mentioned that the Gaussian quadrature, for the same problem, obtained only the relative heating pattern for $y = 0$, $x \geq 0$. Data transmission with the subroutines is via labeled common.

```
      PROGRAM(INPUT,OUTPUT,PUNCH,TAPE5=INPUT,TAPE6=OUTPUT,TAPE7=PUNCH)
      DIMENSIONXIST(64,64)
      DIMENSIONIMAGE(900),XM(64),D(101)
      DIMENSION NUM(64,6),NNP(6),NRANG1(32,6),NRANG2(32,6),NLOOPS(6)
      DIMENSION NUNSC(64),NN(12),NM(12),NNX(64)
      COMPLEX XT(64,64)
      COMPLEX WEXP,WW
      COMPLEX X(64),XP(64),W(32),XN1,XN2
      COMPLEX AJ,E1,E2,AKSQE1,AKSQE2,EX,OUTPUT
      INTEGER GAMMA,GAM2,A,AN
      COMMON /BLOCK1/ NUM,NNP,NRANG1,NRANG2,NLOOPS,NUNSC,NN,NM,NNX,W
      COMMON /BLOCK2/ GAMMA,GAM2,NDATA,NDAT
      COMMON /BLOCK3/ XT,X,XP
      COMMON/PICKON/C,PI,PI2,PI22,AJ,E1,E2,AK,AKSQ,AKSQE1,AKSQE2,AKATEM
     1AKRTEM,AKSQEF,Z1,Z,V,U,EX,INDEX,OUTPUT,AED,BED
      PI=3.14159265358979
      GAMMA=6
      CALL NUMGEN
      C=2.998E10
      PI2=PI*2.0
      PI22=(PI*0.5)**2
      AJ=CMPLX(0.,1.)
      YY=0.0
      PX=0.0
      PY=0.0
      DELX=0.4999999999
      DELU=2.*PI/(NDATA*DELX)
      DELV=DELU
      PID=-DELU*63./2.
      D(1)=-32.*DELX
      DO 47 M=1,100
47    D(M+1)=D(M)+DELX
      XMIN=D(1)
      XMAX=D(101)
      YMIN=0.0
      DO 82 MA =1,2
      READ(5,305)FMC,EM,TM,EF,TF,Z1,AA,BB
      AED=AA/2.
      BED=BB/2.
```

```
      FMEG=FMC
      FMC=FMC*10.**6
      WRITE(6,302)AED,BED,EM,EF,TM,TF,Z1,FMC,DELX
      E1=EF*(1.0-AJ*TF)
      E2=EM*(1.0-AJ*TM)
      AK=2.*PI*FMC/C
      AKSQ=AK*AK
      AKSQE1=AKSQ*E1
      AKSQE2=AKSQ*E2
      AKRTEF=AK*SQRT(EF)
      AKRTEM=AK*SQRT(EM)
      AKSQEF=AKSQ*EF
      SIGRAT=EF*TF/(EM*TM)
      Z=Z1
      YMAX=0.0
      DO 503 J=1,64
503   XM(J)=0.0
      DO71M=1,64
      DO71N=1,64
71    XIST(M,N)=0.
      AMAX=0.0
      DO 81 NMN=1,3
      INDEX=NMN
      V=PID
      DO 45 M=1,64
      U=PID
      DO 44 N=1,64
      CALL SCRPEX
      CALL JAMXX
      XT(M,N)=OUTPUT
44    U=U+DELU
45    V=V+DELV
      CALL FAST
      WRITE(6,304)Z,INDEX
      DO 70 M=1,64
      DO 70 N=1,64
      XIST(M,N)=XIST(M,N)+CABS(XT(M,N))**2
70    CONTINUE
81    CONTINUE
```

```
      YMAX=XIST(33,33)
      DO 82 N=33,53,2
      DO46 M=1,64
      XM(M)=XIST( N,M)/YMAX
      IF(XM(M).GT.AMAX)AMAX=XM(M)
46    CONTINUE
      IF(Z.GE.Z1)GOTO510
      DO 500 M=1,NDATA
500   XM(M)=SIGRAT*XM(M)
      IF(XM(M).GT.AMAX)AMAX=XM(M)
510   CONTINUE
      IMAX=AMAX
      AMAX=IMAX+1
      YY=D(N)
      WRITE(6,899)
      WRITE(6,306)YY
      CALL PLOT 2(IMAGE,XMAX,XMIN,AMAX,YMIN)
      CALL PLOT 3(1H*,D,XM,64)
      CALL PPLOT4(20,20H  RELATIVE HEATING                    )
      DO 501 M=1,64
      WRITE(6,303)M,XM(M)
501   CONTINUE
      DO 504 M=13,53
      IFH=2
      IF(M.LT.33)IFH=1
      XX=D(M)
      IF(M.LT.33)XX=-D(M)
      WRITE(7,300)  XX,YY,Z,PX,PY,XM(M),FREQ,Z1,IFH
504   CONTINUE
      IF(Z.EQ.Z1)Z=-0.9
      IF(Z.LT.0.5.AND.Z.GT.0.0)Z=0.0
      Z=Z+0.5
      IF(Z.EQ.Z1)Z=Z+0.5
82    CONTINUE
```

```
  301   FORMAT(3F6.2,3F12.6,F10.3,F7.3,I3)
  302   FORMAT(5H A = ,F10.3/5H B = ,F10.3/8H EPSM = ,F10.3/8H EPSF = ,
     1F10.3/8H TAUM = ,F10.3/8H TAUF = ,F10.3/6H ZI = ,F10.3/
     18H FREQ = ,E12.3/11H DELTA X = ,F10.3)
  303   FORMAT(4(I10,F20.10))
  304   FORMAT(1H0,4HZ = ,F5.2,10X,8HINDEX = ,I3)
  305   FORMAT(8F10.5)
  306   FORMAT(1H1,5H Y = ,F6.3)
  399   FORMAT(1H1)
        STOP
        END
```

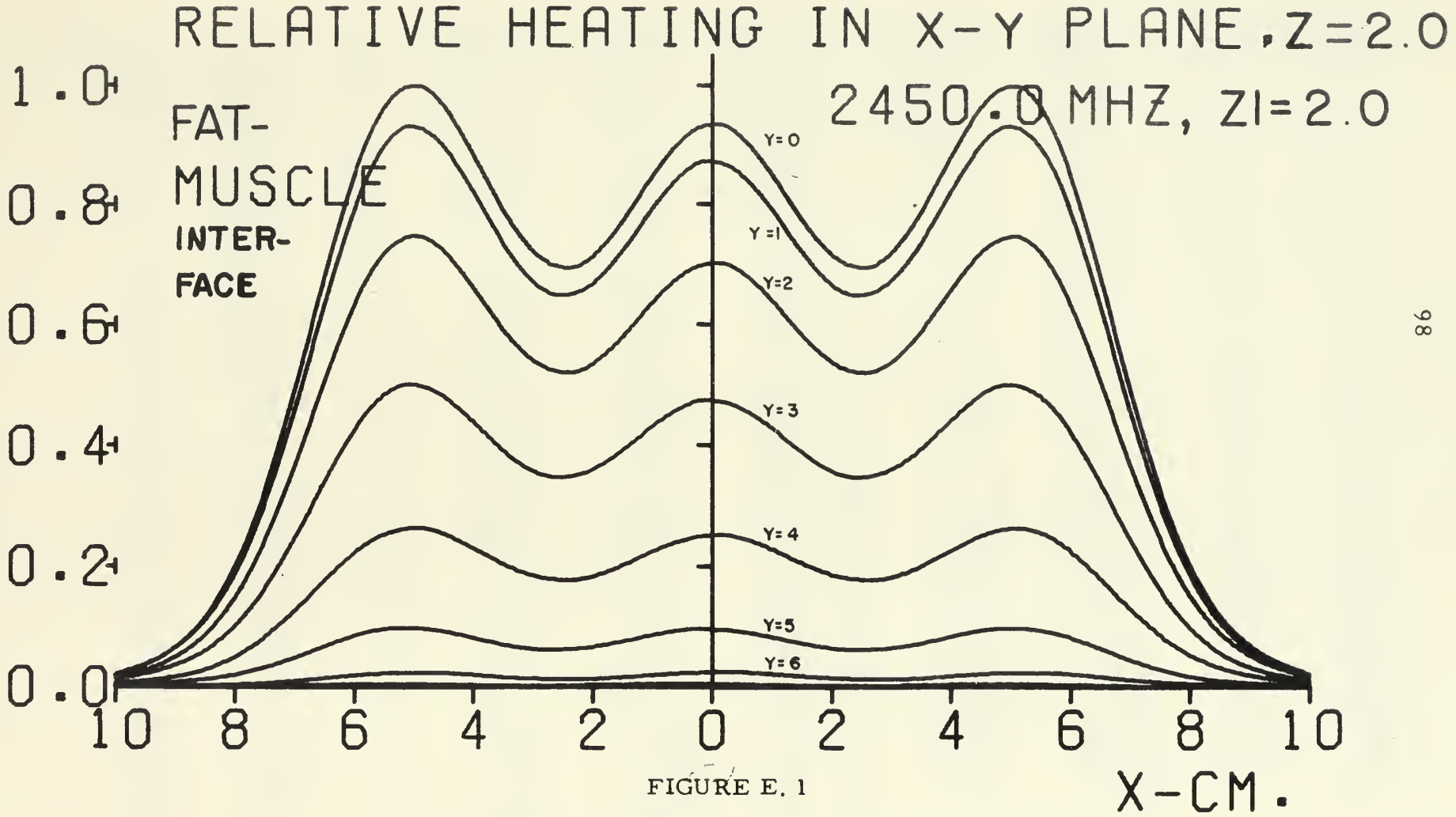

FIGURE E. 1

2450 mHz Fat-muscle Interface RHP with Y Varied

BIBLIOGRAPHY

1. Licht, S. "History of Therapeutic Heat." Therapeutic Heat. Licht, S. (ed.). 2d ed. Baltimore: Waverly Press Inc., 1965, pp. 196-231.

2. Moon, F. B. "Microwave Diathermy." Therapeutic Heat. Licht, S. (ed.). 2d ed. Baltimore: Waverly Press Inc., 1965, pp. 310-320.

3. Guy, A. W. et al. "On the Determination of an Optimum Microwave Diathermy Frequency for a Direct Contact Application," IEEE Transactions On Bio-Medical Engineering, vol. BME - 13:2, pp. 76 - 87, April, 1966.

4. Guy, A. W., Lehmann, J., et al. "Studies on Therapeutic Heating by Electromagnetic Energy," Thermal Problems in Biotechnology. New York: American Society of Mechanical Engineers, 1968, pp. 26-45.

5. Guy, A. W., Lehmann, J. "Comparative Evaluation of Electromagnetic Diathermy Modalities in 433 mHz to 2450 mHz," Proceedings of the Annual Conference on Engineering in Medicine and Biology. Houston: McGregor and Werner, Inc., 1968, p. 19.2.

6. U. S. Congress. Senate. Committee on Commerce. Radiation Control for Health and Safety Act of 1967. Hearing, 90th Cong., 1st Sess., August 28 - 30, 1967. Washington: Government Printing Office, 1968.

7. U. S. Congress. Senate. Committee on Commerce. Radiation Control for Health and Safety Act of 1967. Hearing, 90th Cong., 2nd Sess., May 6 - 15, 1968. Washington: Government Printing Office, 1968.

8. Lazell, J. A. "Radiation Control for Health and Safety Act of 1968," Health Physics, vol. 16, pp. 525-526, 1969.

9. Susskind, C. (ed.). "Preface," Proceedings of the Third Annual Tri-Service Conference on Biological Effects of Microwave Radiating Equipments. Berkeley: University of California, 1959, p. v.

10. Schwan, H. P. "Biophysics of Diathermy." Therapeutic Heat. Licht, S. (ed.). 2d ed. Baltimore: Waverly Press Inc., 1965, pp. 63 - 125.

11. Guy, A. W., and Lehmann, J., "Quantitative Methods for Analyzing Electromagnetic Fields and the Associated Heating Patterns in Human Tissues," Summaries of the Fourth IMPI Symposium, Waterloo: University of Waterloo, 1969, pp. 45 - 53.

12. Villeneuve, A. T. Admittance of Waveguide Radiating into Plasma Environment. Scientific Report No. 6. Cambridge: Air Force Cambridge Research Laboratories, October, 1968, pp. 13-18.

13. Guy, A. W. et al. "Quantitative Methods for Analyzing Electromagnetic Fields and the Associated Heating Patterns in Human Tissues," To be published in the IMPI Journal, Spring 1970.

14. Morse, P. M., and Feshbach, H. Methods of Theoretical Physics. Part 1. New York: McGraw-Hill Book Company, 1953, pp. 452 - 471.

15. Bracewell, R. M. The Fourier Transform and Its Applications. New York: McGraw-Hill Book Company, 1965.

16. Cooley, J. W., and Tukey, J. W. "An Algorithm for the Machine Calculation of Fourier Series," Math. of Comput., vol. 19, pp. 297 - 301, April 1965.

17. Cooley, J. W. et al. "Applications of the Fast Fourier Transform to Computation of Fourier Integrals, Fourier Series, and Convolution Integrals," IEEE Transactions on Audio and Electroacoustics, vol. AU - 15:2, pp. 79 - 84, June, 1967.

18. Brigham, E. O., and Morrow, R. E. "The Fast Fourier Transform," IEEE Spectrum, pp. 63 - 70, December, 1967.

19. Gentleman, W. M. and Sande, G. "Fast Fourier Transforms - For Fun and Profit," AFIPS Con. Proc. - 1966 FJCC. San Francisco: Spartan Books, 1966, pp. 563 - 578.

20. Bergland, G. D. "A Guided Tour of the Fast Fourier Transform," IEEE Spectrum, pp. 41 - 52, July 1969.

21. Eguchi, R. G., and Carlson, F. P. Coherent Optical Gradient System. Technical Report No. 127. Seattle: University of Washington, November 1968, pp. 71 - 76, p. 82.

22. Singleton, R. C. "A Method for Computing the Fast Fourier Transform with Auxiliary Memory and Limited High-Speed Storage," IEEE Transactions on Audio and Electroacoustics, vol. AU 15:2, pp. 91 - 98, June 1967.

23. Ho, H. S. et al. "Electromagnetic Heating Patterns in Circular Cylindrical Models of Human Tissue," Proceedings - 8th ICMBE Chicago: Palmer House, 1969, p. 27.4.

Thesis
S2455 Schaefer
Application of the fast Fourier system to the computation of electric fields and associated heating patterns in human tissue.
112683
19 JAN 70
DISPLAY

Thesis
S2455 Schaefer
Application of the fast Fourier system to the computation of electric fields and associated heating patterns in human tissue.
112683

thesS2455
Application of the fast Fourier system t
3 2768 001 00412 0
DUDLEY KNOX LIBRARY